Technical Report

TR-99-11

Water exchange of Öregrundsgrepen

A baroclinic 3D-model study

Anders Engqvist

A & I Engqvist Konsult HB, Vaxholm

Oleg Andrejev

Finnish Institute of Marine Research, Helsinki

April 1999

Svensk Kärnbränslehantering AB
Swedish Nuclear Fuel
and Waste Management Co
Box 5864
SE-102 40 Stockholm Sweden
Tel 08-459 84 00
+46 8 459 84 00
Fax 08-661 57 19
+46 8 661 57 19

Water exchange of Öregrundsgrepen

A baroclinic 3D-model study

Anders Engqvist
A & I Engqvist Konsult HB, Vaxholm

Oleg Andrejev
Finnish Institute of Marine Research, Helsinki

April 1999

Keywords: Numerical model, 3D, baroclinic, cascaded coupling, grid, water exchange, retention time, SAFE, SFR, Öregrundsgrepen, Baltic Sea.

Abstract

Hypothetically possible transport of radionuclides from the SFR repository could also be mediated by natural water circulation within receiving coastal basins. In this context a basic equation, free surface 3D-model has been used to compute the water exchange of the Öregrundsgrepen bay-like area for a representative full year cycle. This has been achieved in two steps in order to provide coherent densimetric and sea level elevation boundary data relative to the adjacent Baltic coastal water. Weather data from 1992 were chosen. The focus is placed entirely on water exchange aspects with no consideration of what the water parcels may contain. Earlier model and measurement programs have also been reviewed.

The **first phase** consisted of running a 3D-model encompassing the entire Baltic Sea. This model resolves the Baltic horizontally in five by five nautical miles (5'×5'). This model was driven by gridded (approx. 20'×20') synoptic weather data with geostrophic wind and the varying density and sea level elevation on the Kattegat border. Freshwater discharge from the major rivers along the Baltic coastline was also taken into account. Initial data prior to December 1991 have been assessed from the available, but relatively scarce, salinity and temperature profile measurements in the Baltic. The time step was 2 hours. The relevant boundary data in the vicinity of the Öregrundsgrepen area were saved after one full-year cycle of simulation.

The **second phase** consisted of running a local model over the Öregrundsgrepen with a higher horizontal grid resolution consisting of a 0.1'×0.1' grid. This model was driven by the same weather data, combined with the saved densimetric and sea level elevation boundary data that were produced by the Baltic model with the coarser grid. This procedure applies both for the wide northern and the narrow southern interface. The transference of boundary data necessitated development of an appropriate interpolation scheme. This model has also been run for a full-year cycle allowing one month (December 1991) of spin-up time. The time step has been varied between 3 and 6 minutes.

The retention time of the Öregrundsgrepen was found to vary between 12.1 days (surface) and 25.8 days (bottom) as a yearly average.

Special regard has been placed on estimating the ventilation of a particular subarea where a biological model study is currently being performed. This subarea is located in the waters above the SFR-depository embedded within the Öregrundsgrepen model area. The exchange intensity, expressed as a yearly average transit retention time, spanned from 0.5 days (surface) to 1.2 days (bottom) with regard to the depth strata that the model resolves. The bulk volume average for all strata was 0.77 days with a standard deviation of 0.22 days equally for both intra-monthly and inter-monthly variations. The corresponding average total volume flow across the boundary was 2.1×10^3 m^3/s.

Sammanfattning

Mot bakgrund av en hypotetiskt möjlig vattenflödesburen transport av radionuklider från SFR-förvaret har en numerisk 3D-model, baserad på grundläggande hydrodynamiska ekvationer utnytttjats för att beräkna vattenutbytet i Öregrundsgrepens buktliknande område för en representativ komplett årscykel. Detta har åstadkommits i två steg för att tillgodose kravet på samstämmig drivning såväl för täthetsbaserade variationer på randen mot Östersjön som för vattenståndsfluktuationerna. För den atmosfäriska drivningen utvaldes bland tillgängliga data de från 1992. Studien avser enbart vattenutbytet. Tidigare modellstudier och mätprogram i området har även granskats.

Den **första fasen** bestod av att simulera hela Östersjöns cirkulation för ett genomsnittsår. Denna modell upplöser Östersjön horisontellt i ett fem gånger fem distansminuter stort (5'×5') rutnät. Denna modell drevs av väderdata avseende 1992 bl a innehållande geostrofisk vind som beräknats i rutnätspunkter med grövre (c:a 20'×20') horisontell upplösning. Vidare bestod drivningen av genomsnittliga täthetsvariationer och vattenståndsfluktuationer i modellens rand vid Kattegatt. Genomsnittlig sötvattentillrinning från de stora älvarna och floderna har också inkluderats. Begynnelsetillståndet vad gäller skiktningen före december 1991 har sammanställts från de relativt fåtaliga tillgängliga salinitets- och temperaturdata i Östersjön för de tre sista månaderna 1991. Tidssteget uppgick till 2 timmar. De framräknade gränsdata i Öregrundsgrepens närhet sparades med full tidupplösning för hela årscykelsimuleringen.

Vid den **andra fasen** användes en lokal modell över Öregrundsgrepsområdet. Denna hade en avsevärt högre horisontell upplösning där beräkningscellernas sida var 0,1'×0,1'. Denna modell tilläts drivas av samma väderdata som ovan i kombination med de täthetsprofiler och vattenståndsdata, som framräknats av Östersjömodellen med den grövre rumsupplösningen. Detta avser såväl den norra som den södra randen. Överföringen mellan modellerna av dessa randdata krävde utvecklandet av ett interpolationsberäkningsschema. Denna modell kördes också för en hel årscykel med en månads inkörningstid (december 1991) för att åstadkomma så korrekta dynamiska initialvärden som möjligt. Tidssteget för beräkningarna varierade mellan 3 och 6 minuter. Uppehållstiden för vattnet i Öregrundsgrepen befanns som ett årsgenomsnitt variera mellan 12,1 dygn (ytlagret) och 25,8 dygn (bottenlagret).

Speciell hänsyn har tagits till att uppskatta ventilationen för det delområde där en biologisk modelleringsstudie genomförs. Detta är lokaliserat till vattenområdet ovanför SFR-förvaret. Framräknade utbytesintensiteter uttryckt som genomsnittlig transient uppehållstid varierar mellan 0,5 och 1,2 dygn med avseende på de djuplager som modellen upplöser. Volymskorrigerad medelutbytestid för samtliga lager befanns uppgå till 0,77 dygn med en standardavvikelse av 0,22 dygn både för genomsnittliga variationer inom som mellan månader. Motsvarande sammantaget volymflöde över biomodellområdets gräns uppgick till $2{,}1\times10^3$ m^3/s.

Contents

1 Introduction

1.1 Relationship to "safe" reporting context

This report is a part the SKB project "SAFE" (Safety Assessment of the Final Repository of Radioactive Operational Waste). The aim of project SAFE is to update the previous safety analysis of SFR-1. The analysis should be presented to the Swedish authorities not later than in year 2000. SFR-1 is a facility for disposal of low- and intermediate-level radioactive waste, which is situated in bedrock beneath the Baltic Sea, 1 km off the coast near the Forsmark nuclear power plant in the northern part of the province of Uppland.

The SKB reports "Project SAFE – Update of the SFR-1 safety assessment Phase 1" (Andersson et al. 1998a) and "Project SAFE – Update of the SFR-1 safety assessment Phase 1 Appendices" (Andersson et al. 1998b) present an overview of the SAFE project as well as the work that needs to be performed to achieve the goal of the project.

1.2 General considerations

The Öregrundsgrepen area (see Fig. 1) cannot strictly be regarded as a proper bay since it is connected at its southern end by a canal-like channel in which through-flow occurs. The bay-like impression prevails, however, when comparing the section areas of the northern and the southern entrances, which gives a quotient of about 70. In the following this entire study area will referred to as *ÖG* for brevity. An attempt to explain the physical interpretation of some basic oceanographic terms presently used may be found in Engqvist (1997).

The water turnover in the ÖG area has in the past been studied and modelled using many different approaches. The influence of the cooling water of the nuclear plants has then been put in focus. A rough estimate based on data from Hemström (1993) gives that the typical heat contribution of the cooling water from the reactors, if distributed over one tenth of the entire ÖG area, is in parity with the average daily net insolation. In the near-field this certainly means a significant influence on the heat dynamics. The present study differs in this respect as *the basic assumption is that the nuclear plants are shut off* and the water circulation and heat dynamics are driven by the forcing that would ensue after their closure. The presented water turnover estimates are thus supposed to be valid for a projected near-future year when the reactors are closed and the discharge of surplus heated water has completely ceased.

The water exchange of the biomodel (BM) area, located in the central part of the ÖG area (Fig. 1), has been the major objective of this study. In order to achieve a realistic assessment of its water exchange, the whole area with its varying topography must be included in the study. In addition to the local wind forcing, the densimetric variations in the adjacent Baltic coastal water are also deemed to be of great importance for the water turnover. Since densimetric measurements (combined salinity and temperature) data are not available with any acceptable temporal resolution, this in turn has necessitated a whole-Baltic model to be employed in order to provide the boundary data for the model of this locally restricted ÖG area.

The overruling ambition has been to provide an estimate of the water exchange during a typical year cycle. Statistically derived synoptic weather data sets that fulfil reasonable

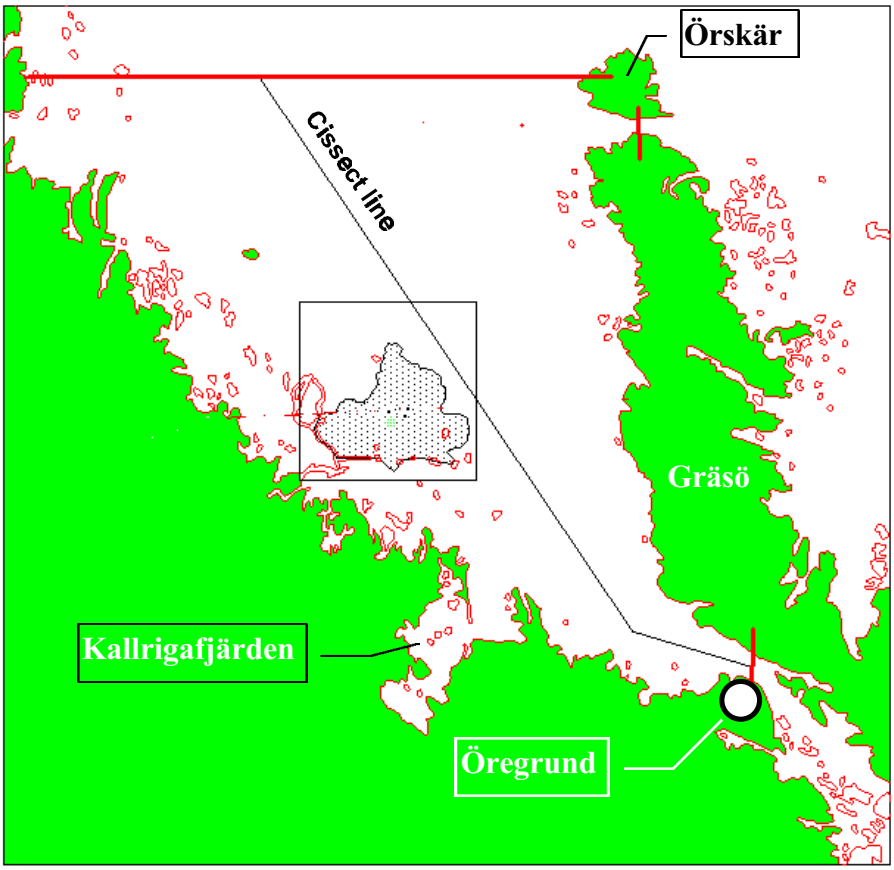

Figure 1. *Map over Öregrundsgrepen (ÖG) with some local names indicated. The ÖG-model area is delimited by coarse lines. The position of the irregularly shaped biomodel (BM) area is located by the square in the centre. A cross-section (more appropriately named cissect line) along the bay axis is indicated for subsequent references.*

requirements of normality have only quite recently been made available. Even so, it seems safe to state that among meteorologists there does not exist any strong consensual opinion over what constitutes a normal weather year. The difficulty is underscored by the accumulating evidence of ongoing global changes in the climate. After having considered various approaches, it was decided to choose a year that at least could not be discarded as obviously atypical. The choice fell on 1992.

The central presupposition of dismissing the thermal influence of the nuclear reactors has two immediate consequences: one favourable, the other not. That the thermal plume thus may be exempted from the model is certainly favourable from a computational point of view and is obviously motivated in that it also facilitates possible future comparisons with altered climatological factors. By the same token, however, the possibility to validate the model with actual measurement data becomes diminished. This applies certainly in the first place to the temperature variations, but also indirectly to the salinity and to a lesser degree even to the velocity fields. The accessible data for such validation during the study year 1992 turned out to be limited (see Chapter 4) which mitigates the shortcomings in this regard.

When referring to salinity measurements, the PSU-scale (Unesco, 1985) has been used consistently if not otherwise noted. For most practical purposes this scale mainly coincides with the earlier used permille (ppt) measure.

1.3 Organisation of the present report

The present report is organised as follows: first a brief account of earlier investigations is given together with a description of the area's hydrography. Then follows an inventory of the physical forcing and available data thereof. The 3D-model equations are then given in their mathematical formulation, together with a brief description of the numerical features of the model. The mathematical aspects have been toned down and the emphasis has been placed on presenting a description of the oceanographical considerations for the model design. Finally the model results and their inherent turnover estimates are presented. These results are discussed as to their realism and accuracy in the context of intra-monthly and inter-monthly variations. A short summary of major findings concludes the paper.

2 Earlier investigations

The hydrography of the ÖG area has been studied since the early 1970s. The measurement program has mainly been conducted by SMHI (Swedish Meteorological and Hydrological Institute). Inferred from publication lists, the intensity seems to have culminated about 1975. In the following decade the first numerical circulation model studies of this area were performed. A survey of these efforts follows.

2.1 Model studies

To the present authors' knowledge, the first attempt to quantify the water exchange of the ÖG area was performed by Sundblad et al. (1983). This study was regretfully not explicit about the hydrological methods used. It could be inferred that it was inspired by Evans (1985) who used a box-model approach by partitioning the entire Baltic Sea into 12 (depicted) to 25 (stated in text) homogeneously mixed boxes both vertically and horizontally. Furthermore, an underlying assumption was that a steady-state condition with regard to constant sources prevailed. This relegates the validity of this approach to time scales long enough to cancel episodic variations (i.e. applicable for decades and longer) as to cancel inter-annual variations. The steady state was studied using radioactive material with known rates of decay. Sundblad et al. (1983) partitioned the ÖG area into eight such well-mixed boxes.

The predictions of this box-model approach were checked by Gidhagen and Rahm (1990) using a 3D-hydrodynamic equation solver PHOENICS (Spalding, 1981) that resolved the ÖG area in 69×35 grid cells horizontally and 8 vertical layers. Full advantage of the basin-fitted coordinate facility was taken. This model was designed with an open boundary feature, remotely located about the same distance from the Örskär-mainland cross-section in the east, north and west directions as this section is wide. This model was also run in a steady-state mode with constant artificial wind data projected in three predominant wind directions. The water transports across the above-mentioned box model (i.e. Sundblad et al., 1983) boundaries were recalculated and the corresponding retention times were compared to the box model estimates. The disparity of these estimates was striking and displayed a relative difference amounting to an order, in a few cases orders, of magnitude.

In a subsequent modelling effort by Gidhagen, Nyberg and Rahm (unpubl.), the steady-state assumption was replaced by a fully time-dependent deployment of the same model and with identical grid resolution. This study was validated against historical velocity data recorded in 1970. The outcome of this validation was that the model tended to overestimate the measured currents, but showed a capacity to convincingly capture the response to shifting wind forcing. This model was subsequently used to study dispersion of waterborne particles, and was founded on a further elaboration of sediment dynamics presented by the same authors (Gidhagen et al., 1989).

All of the modelling efforts mentioned above were flawed by a central and hypothetically important factor: neglecting the influence of vertical density variations on the border. Following Stigebrandt (1990), it is well established that what concerns the ventilation of other Baltic coastal areas (Engqvist, 1990; Engqvist & Omstedt, 1992, Engqvist, 1993 and Engqvist 1996), the baroclinic exchange associated with coastal up-/downwelling

events, has a strong – in many instances even dominant – influence on the water exchange. The importance of this mechanism is underscored by the wide open northern boundary of the Öregrundsgrepen that also lacks a sill threshold that would restrain entering denser water from flowing back out again. The rationale for neglecting this baroclinic mode of water exchange was that the vertical density differences are typically small.

Hemström (1993) used the same above-mentioned hydrodynamic equation solver PHOENICS to compute the stationary response to constant wind forcing utilising a body-fitted grid that resolved the ÖG area into 8 layers vertically and 71×51 grid cells horizontally. Part of this study was aimed at elucidating the consequences of a projected deployment of current inducers in order to facilitate the spreading of the reactor cooling water. The ensuing model results with the current inducers absent, in spite of being admittedly unrealistic because of the steady-state assumption, were compared to actual measurements of current velocities and salinity and temperature profiles. The evaluation of these data is deferred to the next section.

Even though the stratification in the ÖG area is arguably weak, a separate study (Engqvist, 1999) demonstrated that the known average density fluctuations recorded on a 10-year time period suffice to produce retention times of the same order of magnitude as the purely wind-driven exchange of Gidhagen and Rahm (1990).

2.2 Empirical field investigations

An attempt to estimate the water turnover in the isolated depths was made by Lindell and Kvarnäs (1978), and was based on dye-injection experiments at two sites at 47- and 45-m depths. It was found that the dye (rhodamine) on the two measurement occasions (1978-08-15 and 1978-08-16) was flushed away from the deep cavities in a time period of less than 24 h. Temperature profiles were measured at five sites along the deep trench to the east of centre line of the ÖG bay in the north/south. Current profiles were also recorded with gelatine pendulum meters. It is interesting that the mean current velocity for one accounted station showed a maximum intensity for 35–40 m depth interval.

Swedish Meteorological and Hydrological Institute (SMHI) has conducted oceanographical surveys in the ÖG area since 1971. The year 1992 was no exception, and the collective effort has been compiled by Andersson and Hillgren (1993). From the perspective of finding data for possible validation purposes of the circulation model results, the potentially most useful data presented are two temperature contour diagrams (depth vs. time) spanning the periods 1992-06-02 to 1992-06-22 and 1992-10-13 to1992-10-31. It is mentioned that these measurements, however, to some extent were perturbed by cooling water from a reserve outlet discharge. This report also contains a detailed map over the ice cover extension 1992, which subject will be returned to in section 3.3.

In the context of validating a 3D-model run in stationary mode, Hemström (1993) undertook with the assistance of SMHI, simultaneous salinity, temperature and current velocity measurements by deploying recording CTD-meters at three different sites. At one of these sites, two different depths were covered. These measurement were performed 1992-07-09 through 1992-09-03. The resulting current measurements were presented as “current roses,” that is, depicted in polar coordinate frequency diagrams. The most promising of these data for validating purposes is the salinity data series that compares the recorded salinity at two nearby sites, one at a depth of 3.5 m, the other at 10.6 m.

3 Hydrography of the Öregrundsgrepen

The ÖG area may be roughly described as a flattened funnel with its wide opening toward the north and connected to the south through the silled narrow strait at Öregrund (see map Fig. 1). The east side of the major embayment has a deeper side east of a symmetry line with isolated depths exceeding 40 m. The coastline on either side is ragged and artificially constructed road banks and other embankments add to the complexity of the bottom topography.

3.1 Freshwater discharge

There are four streams that discharge freshwater into the area, but even the maximum monthly averaged flow of the largest one amounts merely to about 10 m^3/s. The two major streams, Olandsån and Forsmarksån, discharge into the same minor embayment, Kallrigafjärden, and their combined flux is deemed to have a locally restricted effect by driving an estuarine circulation at the location of the discharge area. Since the freshwater content of the water flushed across the boundaries is several orders of magnitude greater, the influence by these greater streams on the general circulation of the ÖG area is small to the point of being negligible. Despite this, for the sake of completeness, they have been included in the modelling with a monthly temporal resolution in order to resolve their possible local influence. The other two even smaller streams (Böleån and Sladaån) discharge outside the northern boundary and are thus neglected.

The mean direct precipitation into the ÖG area amounts to 700 mm/yr. Allowing for an evaporation rate of 400–500 mm/yr, the runoff amounts to about 200–300 mm/yr, with a standard deviation of ± 100 mm/yr (Tobias Lindborg, pers. comm). With a surface area of approximately 400 km^2, this amounts to a mean freshwater source of about 10 m^3/s (i.e. comparable to the run-off of the streams). This precipitation amount is however distributed over the the entire ÖG area, and for the same argument as for the stream discharge it may thus be ignored.

3.2 Exchange mechanisms

For an explanation of the oceanographic nomenclature used in this section, the interested reader may consult Section 4 in Engqvist (1997) which deals with water exchange in the coastal waters surrounding the Äspö island. A similarity between this earlier study and the water exchange in the ÖG area is that the intermediary circulation (*sensu* Stigebrandt, 1990), constitutes a dominating mode of exchange. This type of exchange is induced by the densimetric fluctuations of the adjacent Baltic coastal water induced by up-/down-welling events due to Ekman dynamics when along-coast winds transport surface coastal water sea-/coastwards. The densimetrically induced intermediary circulation is enhanced in this case by the wide cross-section of the northern interface and the absence of any marked sill. The northern boundary is normally much wider than the internal Rossby radius and thus one expects rotational effects to be manifested in the northern part of the area. This phenomenon is routinely handled as an intrinsic part of the present model's construct. Departing from the estimate of the average retention time of 5 days and a volume of 5.8 km^3 for the entire ÖG area (Engqvist, 1999), the dominating baroclinic exchange of this study translates into a long-term mean flow of

approximately 13×10^3 m^3/s. Another baroclinic mode of circulation may also occur between shallower and deeper areas, in particular if these are connected by interfaces with wide open section areas. The process of heating/cooling is then much faster in the shallow area which thus induces a baroclinic circulation due to the density difference with regard to depth. According to Söderkvist (1997) this may even be a dominant mode of ventilation of shallow embayments.

The barotropically induced circulation does certainly contribute to the ventilation of the ÖG area water. A coarse estimate may be achieved if 5 cm/day, representing a 10-year mean rate of change of the sea level at 60.5° latitude according to Engqvist (1999), is multiplied with the ÖG surface area of about 400 km^2. This calculation gives a volume flow of 230 m^3/s, which is orders of magnitude smaller than the baroclinically induced flows across the northern boundary. Sea level differences between the northern and southern parts of the ÖG area may be maintained by the prevailing wind regime in combination with temporal geostrophical adjustments of the off-coast circulation resulting in a barotropic flow component through the Öregrund strait with current velocities of considerable magnitude. The mean through-flow has been indicated by Persson et al. (1993) to amount to 540 m^3/s but with no further qualification of the time scale to which this average refers.

3.3 Ice dynamics

Ice formation occurs regularly. On the average an ice cover forms the last week of December and melts by mid-April (Lundqvist & Årnell, 1992). During the study year 1992 ice formation began in the southern part at the end of January, reached its maximum extent northward at Engelska Grundet about halfway to the model border. All ice was gone the third week in March (J-E Lundqvist, pers. comm.). An ice cover considerably reduces wind-mixing and must to be included in the model formulation (Omstedt, 1998). An ice cover also provides an effective thermal insulation from the heat exchange with the atmosphere (Omstedt, 1990; 1999). The heat discharge by the nuclear reactor cooling water are not considered since the basic assumption is that the reactors are shut down.

4 Hypsography and gridding

4.1 The Baltic model grid

The bottom topography compiled by Stigebrandt and Wulff (1987) has been used. This horizontal grid is a mesh with 125 by 145 nodes (including nodes on land). The horizontal resolution is 5 by 5 nautical miles or approximately 10×10 km.

The model domain includes the entire Baltic Sea with the Danish straits and the southern part of the Kattegat. The gridded hypsography is depicted in Fig. 2.

4.2 The Öregrundsgrepen grid

The original grid of the ÖG area has been provided by Lars Brydsten (Brydsten, 1999). The choice of horizontal resolution has been negotiated as a compromise between the need to resolve the relevant hypsographical features that determine the water circulation versus the resulting computational effort which increases at least in direct proportion to the number of grid cells. The final resolution was fixed to be 0.1 nautical mile, approximately 185 m, in either horizontal direction.

This grid is derived from isogonal grid cells. Because of the earth's curvature, the sides of the cells will deviate slightly from being perfect squares. A check as to determine to what extent the grid cells fullfilled the required property of forming a proper square gave that the maximal deviation was less than 1%, which seems fully acceptable.

Originally the ÖG grid was designed to fit snugly to the Baltic grid, but this produced two negative consequences. The first was that an open boundary corner occurred which is detrimental from a numerical scheme point of view. The second was that a host of unnecessary grid points were comprised east of Gräsö. For these two reasons the northern boundary was moved southward to the location indicated in Fig. 3.

Even with this comparatively fine resolution of 0.1', there are some topographical features that could not be resolved. Among these can be mentioned a few minor islands, the road banks surrounding the enhanced water temperature 'Biotest' area and other artificially constructed embankments that certainly block water circulation around the SFR-area.

The first attempt to manually adjust the grid in this respect was abandoned for a better approach. This second approach was originally advanced for preventing the model from running dry on occasions of low sea level. Since the anticipated lowering of the sea level in grid cells near the coast would amount to one meter relative to the nominal sea level elevation, all grid cells that were shallower than one meter have been excluded from the simulations. This adjustment produces a map (see Fig. 3) in which the above-mentioned embankments reappear. By the same token the coastline became less rugged. No further adjustments were needed except for filling "lakes" that are disconnected from the sea. The shallow passage between Gräsö and Örskär was completely filled, since this passage in any case is short-circuited by the overwhelmingly wider northern model interface to the Baltic.

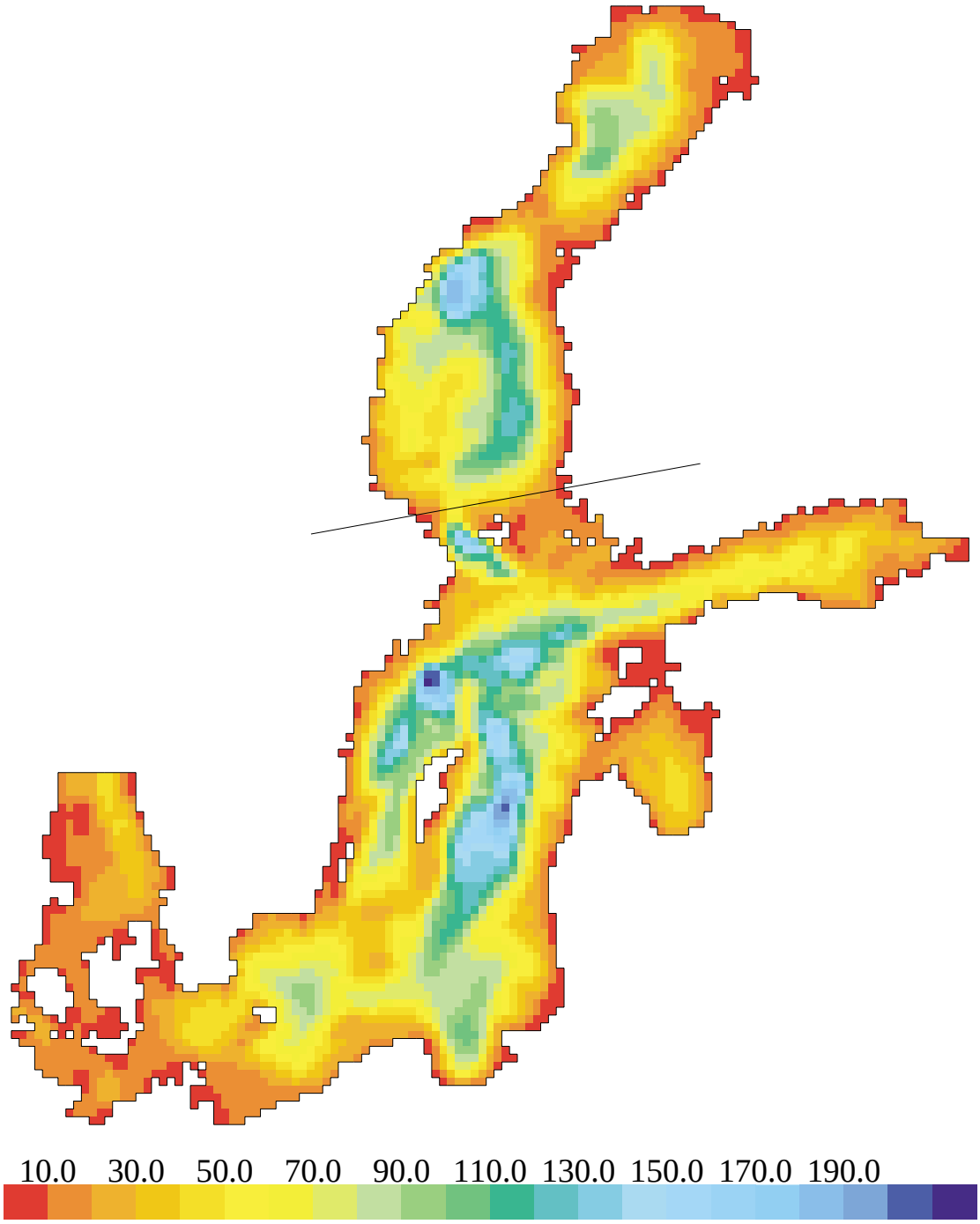

Figure 2. *The Baltic hypsography. A line north of Åland indicates the position of a transect passing through the ÖG area. This transect will be referenced for some cross-sectional plots.*

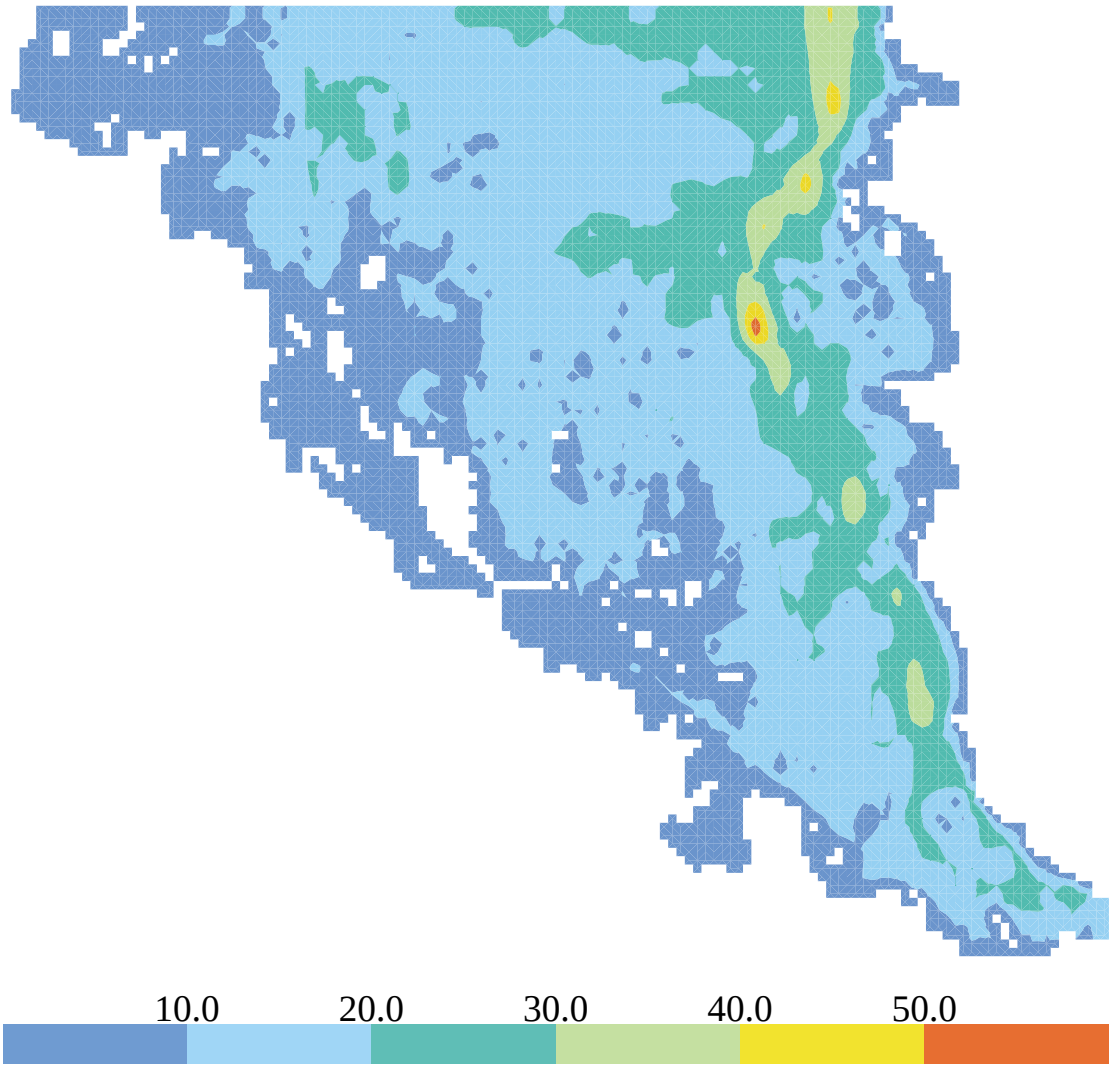

Figure 3. *The hypsography of the ÖG area. The original grid was produced by Lars Brydsten, Umeå University. A cissect along the bay "symmetry" axis is indicated in Fig. 1 for references from Figs. 16 and 17.*

The part of the originally gridded area that maps the northern part of Ängfjärden (south of Öregrund) has been truncated south of the smallest section area of the strait. The motive for this was that the added realism as a buffer area, preserving the hydrographical properties entering or exiting through the southern Baltic interfacial boundary if it were included, was counterbalanced by the added computational effort. The final argument for discarding this section of the original grid was that from a hydraulic point of view, the narrowest parts will mainly determine the flow-through resistance, and not the part where this area widens into several branches.

The final model grid design contains 133×155 grid cells horizontally of which approximately a little more than one half fall on land.

4.3 The biomodel (BM) area grid

The definite delimitation of the BM-area was determined by Lars Brydsten and this recommendation has been adopted into the BM-grid as accurately as possible with only four minor adjustments of the grid location. These adjustments were solely motivated from consideration based on how the numerical model operates: namely that concave, one grid cell-wide periphery border sections are not compatible with computation of the cross-periphery through-flow. The resulting final BM surface area measure remains exactly the same as that originally defined (see Fig. 4). The final hypsography of the gridded BM-area is presented in Table 1.

Table 1. Hypsography of the gridded BM area.

Layer	Depth range	Thickness (m)	No. grid cells	Volume (10^6 m^3)
1	0 m – 2.5 m	2.5	343	29.4
2	2.5 m – 7.5 m	5	301	51.6
3	7.5 m – 12.5 m	5	212	36.4
4	12.5 m – 17.5 m	5	75	12.9

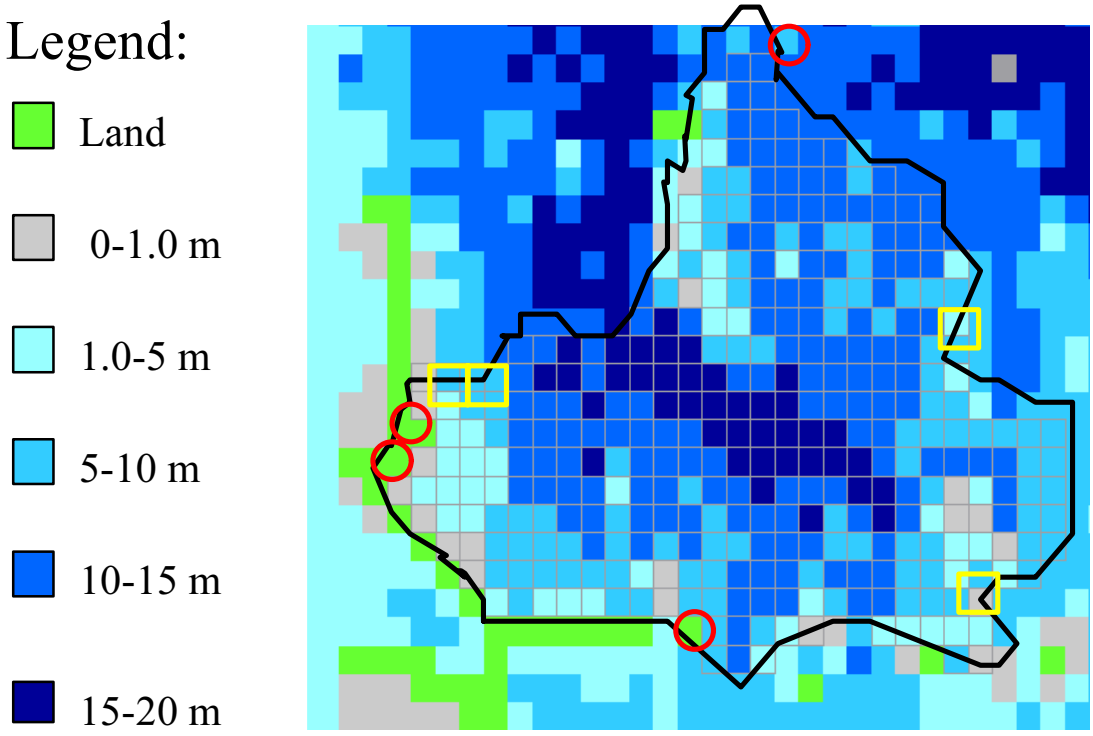

Figure 4. *The hypsography of the BM-area. Note the grid cells with depths between 0-1.0 m are exempted from the model simulations because of the numerical hazard occurring if they should run dry on low sea level occasions. Four grid cells have been shifted on the periphery compared to the original grid. Red circles indicate the omitted ones, yellow squares those added.*

5 Physical forcing data inventory

In the preparation of an encompassing modelling endeavour, a dichotomy between what is desired and what is available often arises. This study is no exception, and the limited time for data acquisition normally becomes the crucial factor. Fortunately this model approach relies mainly on the atmospheric forcing and the local stream discharge data for 1992. Other forcing data are either long-term averages or data that could be used for validation. The latter set has already been commented upon in Section 2.2. Here follows an inventory of the available forcing data.

5.1 Atmospheric forcing

Synoptic atmospheric gridded data with a spatial resolution of 20×20 nautical mile (n.m.), resolve the all-Baltic area in a grid net of 33×23 nodes with a temporal resolution of 3 hours. These data are available for the years 1979 through 1994. An excerpt of this comprehensive data set is given in Fig. 5, in which for each node there are eight synoptically related items of information:

- Air pressure – 900 (hPa)
- N/S-component of geostrophic wind (m/s)
- E/W-component of geostrophic wind (m/s)
- Air temperature (K)
- Humidity (%)
- Cloudiness (%)
- Precipitation (mm)
- Solar radiation (W/m^2)

Since the wind velocity data pertains to geostrophically resolved wind patterns, it differs from the wind at the sea level friction layer. The standard correction is to reduce the wind speed a factor 0.6 and deflect the direction 15° counterclockwise (Bo Gustafsson, pers. comm.). There exists a meteorological station at Örskär in the NE corner of the ÖG study area and random checks, as exemplified in Fig. 6, reveal no reason to perform a closer scrutiny nor any reason to base the local ÖG study on measurement data of local wind.

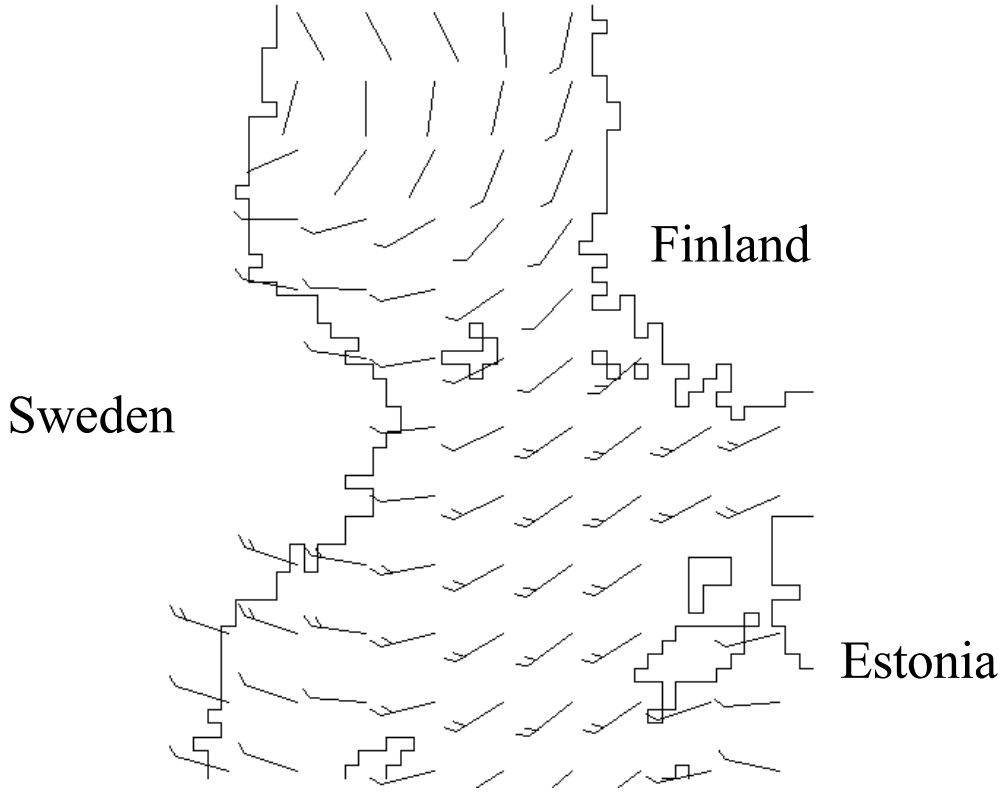

Figure 5. *Synoptic wind velocity 1992-07-01 on the resolved grid points. The symbols are to be interpreted as arrows pointing in the wind direction. The number of small lines at the tail gives the wind speed in accordance with standard meteorological convention.*

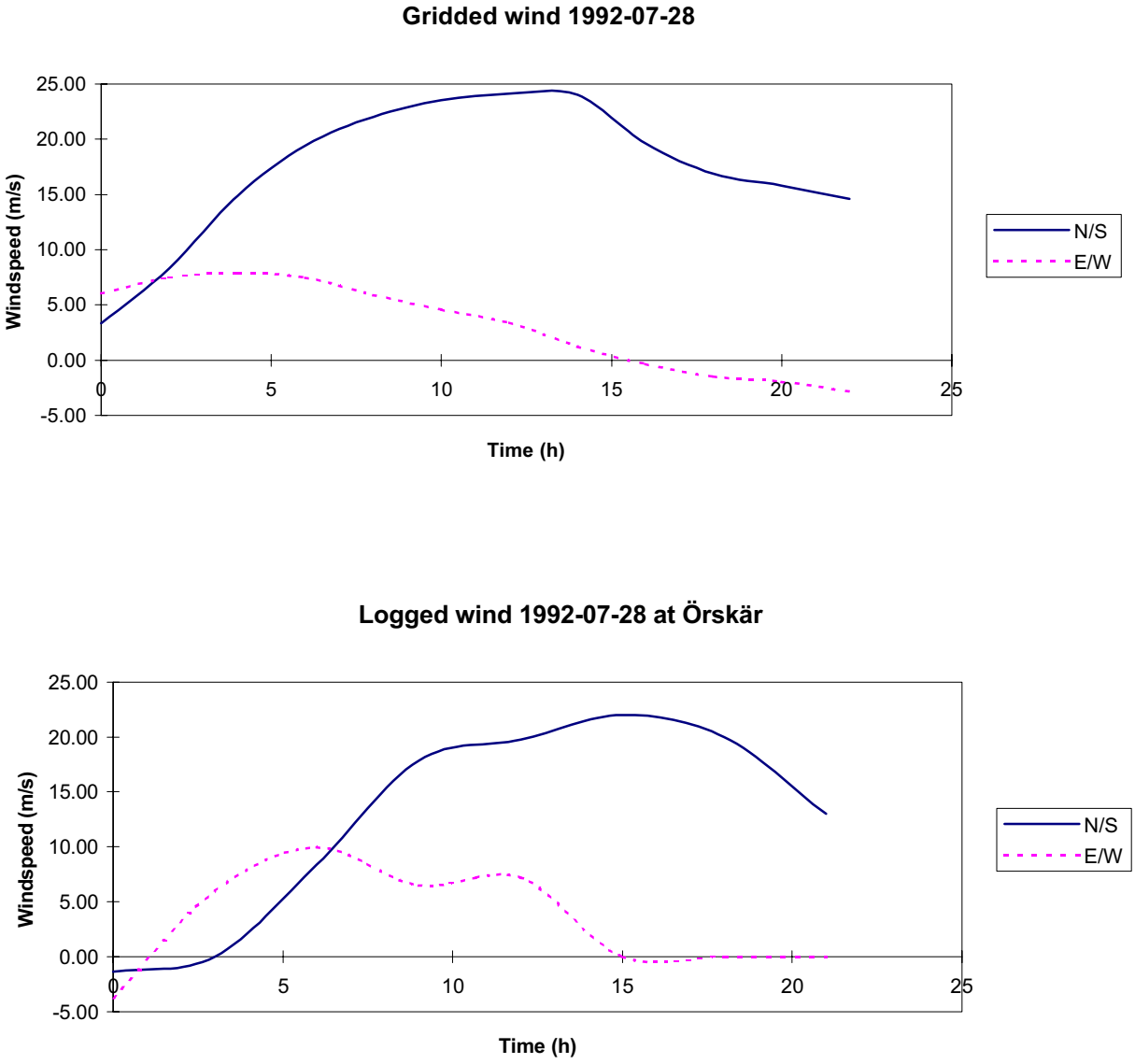

***Figure 6**. Comparison between the N/S- and E/W-components of the adjusted gridded wind (upper diagram) and wind logged 1992-07-28 by SMHI at Örskär. The logged wind is slightly less than the adjusted geostrophic wind but the general similarity is fully acceptable.*

5.2 Hydrological forcing

5.2.1 Baltic boundary data

The modelled densimetric conditions of the Baltic boundary that traverses the southern part of the Kattegat, have been kept very simple: long-term averages of salinity and temperature were maintained throughout the year 1992. The motive for this is that even major episodic saltwater intrusions take considerably longer than one year to manifest themselves on the general dynamics of the Baltic upper layers. This argument particularly applies to the mid-Baltic coasts where the study area is located.

No sea level variation data were acquired.

5.2.2 River discharge of the entire Baltic

These data have been obtained from Bergström and Carlsson (1994) who compiled the river run-off as an average from the years 1950–1970.

5.2.3 Local stream discharge in the ÖG area

The runoff of the four major streams has been estimated from the known discharge of two other streams, Skeboån and Tämnarån, whose runoff has been assessed by SMHI with a monthly resolution. These streams are located north and south of the ÖG area. The runoff per catchment area between these two streams is roughly the same, motivating an estimation of the runoff of the catchment areas in between them using the same net precipitation-evaporation rate. The result is presented in Table 2. Since the study area was curtailed in the northern region, the smallest of these streams (Böleån and Sladaån) no longer discharge into the ÖG model area and may thus be omitted.

Table 2. Run-off data (m^3/s) for the four major streams discharging into the ÖG area.

Stream	Catchment area (km^2)	1991 12	1992 1	1992 2	1992 3	1992 4	1992 5	1992 6	1992 7	1992 8	1992 9	1992 10	1992 11	1992 12
Skeboån	**483**	**1.7**	**1.3**	**1.1**	**4.4**	**6.2**	**4.8**	**0.8**	**0.3**	**0.3**	**0.6**	**1.5**	**5.3**	**6.1**
Gullströmsån	**51**	0.18	0.14	0.12	0.46	0.65	0.50	0.08	0.03	0.03	0.06	0.16	0.55	0.64
Olandsån	**881**	3.10	2.37	2.01	8.03	11.31	8.76	1.46	0.55	0.55	1.09	2.74	9.67	11.13
Forsmarksån	**376**	1.32	1.01	0.86	3.42	4.82	3.73	0.62	0.23	0.23	0.47	1.17	4.12	4.74
Böleån	**70**	0.27	0.21	0.17	0.69	0.98	0.76	0.12	0.06	0.05	0.10	0.24	0.84	0.96
Sladaån	**57**	0.22	0.17	0.14	0.55	0.79	0.61	0.10	0.05	0.04	0.08	0.19	0.68	0.77
Tämnarån	**1258**	**4.8**	**3.8**	**3.1**	**12.3**	**17.6**	**13.6**	**2.2**	**1.0**	**0.9**	**1.7**	**4.2**	**15.0**	**17.2**

5.2.4 Local sea level fluctuations

Since the Baltic model has been demonstrated to compute the local sea level fluctuations from the wind forcing convincingly accurately (Andrejev & Sokolov, 1990), gauged sea level data are necessary only for corroboration purposes. Measurements performed by SMHI from a mareograph located in the vicinity of the Forsmark harbour exist. A comparison between measured and simulated data is deferred to Section 7.3.

6 Model formulation

The model construct is presented in this section. The mathematical formulations – in particular regarding the numerical scheme – have deliberately been put in soft focus. Instead the emphasis has been placed on attempting to communicate the physical ideas behind the formulations. Since the model is based on general hydrodynamical principles, all of the exchange mechanisms mentioned in section 3.2 are entailed.

6.1 General model formulation

The numerical model used in the present study was formulated by Andrejev and Sokolov (1989; 1990). It may be characterised as a time-dependent, free surface, three-dimensional (3D-) model and is as such based on the basic set of governing hydrodynamical (Navier-Stokes) equations:

$$\frac{\partial u}{\partial t}+\frac{\partial uu}{\partial x}+\frac{\partial vu}{\partial y}+\frac{\partial wu}{\partial z}=fv-\frac{1}{\rho_0}\cdot\frac{\partial P}{\partial x}+K_H\Delta_H u+\frac{\partial}{\partial z}\left(K_V\frac{\partial u}{\partial z}\right); \quad (1)$$

$$\frac{\partial v}{\partial t}+\frac{\partial uv}{\partial x}+\frac{\partial vv}{\partial y}+\frac{\partial wv}{\partial z}=-fu-\frac{1}{\rho_0}\cdot\frac{\partial P}{\partial y}+K_H\Delta_H v+\frac{\partial}{\partial z}\left(K_V\frac{\partial v}{\partial z}\right); \quad (2)$$

$$\frac{\partial u}{\partial x}+\frac{\partial v}{\partial y}+\frac{\partial w}{\partial z}=0; \quad (3)$$

$$\rho=\rho(T,S); \quad (4)$$

$$\frac{\partial P}{\partial z}=\rho g; \quad (5)$$

$$\frac{\partial X}{\partial t}+\frac{\partial uX}{\partial x}+\frac{\partial vX}{\partial y}+\frac{\partial wX}{\partial z}=K_H\Delta_H X+\frac{\partial}{\partial z}\left(K_V\frac{\partial X}{\partial z}\right)+F_X; \quad (6)$$

The first two of this set of basic equations denote the momentum balances in x- and y-direction respectively. The velocities in the horizontal direction, defined by an xy-plane, are u and v. In the vertical direction (z-axis) the velocity is denoted w. P corresponds to the local pressure and ρ_o is a reference density (1000 kg/m^3).

K_H and K_V are kinematic eddy diffusivity coefficients in the horizontal and the vertical direction respectively. The former is set constant to 50 m^2/s but the latter varies with depth and is made dependent on the local vertical shear and buoyancy forces according to Marchuk (1980). Finally f is the Coriolis parameter taking into account the effect of rotation. All other external forces, such as wind stress and bottom friction are entered in the form of boundary conditions. The horizontal Laplacian operator is denoted Δ_H.

Equation (3) is the volume conservation equation. The actual small compressibility of water is neglected, which introduces a negligible mass conservation error. The state equation (4) thus also reflects the absence of depth dependence and has been adopted from Millero and Kremling (1976).

Equation (5) takes full account of the vertical density variations, which is not reflected in eq.s (1) and (2). This is often referred to as the Boussinesqian hydrostatic approximation. The gravitational acceleration is denoted g (m/s^2). In eq. (6) finally, X denotes the concentration of the modelled scalar properties that enter (or exit) through the model boundaries or as sources (or sinks) denoted F_X within the model domain. These scalars are *salinity* (S), *heat* ($\rho C_p T$; where C_p is the specific heat for water and T is the temperature) or "*age*" (A). The last item of this triplet denotes the volume-specific transit retention time (*sensu* Bolin & Rodhe; 1973) with the physical dimension ($days/m^3$).

The parametrization of the vertical eddy diffusivity coefficient, K_v , is adapted from Marchuk (1980):

$$K_v = (0.05h)^2 \sqrt{\left(\frac{\partial u}{\partial z}\right)^2 + \left(\frac{\partial v}{\partial z}\right)^2 - \frac{g}{\rho_0}\frac{\partial \rho}{\partial z}}; \qquad (7)$$

The parameter h is set to 2.5 m, i.e. one half of the standard thickness of the top layers (except of the topmost one). The horizontal eddy diffusivity coefficient, K_H, is set to 50 m^2/s for the Baltic simulations and 10 m^2/s for the ÖG area with the finer resolved grid. The relationship between these parameters is theoretically the length-scale raised to 4/3 (e.g. Lam et al., 1984; Tennekes & Lumley, 1972).

6.2 Account of the boundary conditions

Starting with the horizontal sea surface interface with the atmosphere, the drag coefficient, C_{da}, at sea free surface according to Bunker (1977) is:

$$C_{da} = 0.0012(|W|\ 0.066 + 0.63); \qquad (8)$$

where W is a wind velocity. For the bottom friction the drag coefficient, C_{db}, was set to 0.0026. At the free surface the boundary condition prescribes a balance between the turbulently mediated vertical momentum transfer and the rate of momentum production by the wind stress.

The formulation of heat transference at the air-sea interface (Lane & Prandle, 1996) is given as

$$F_T = \frac{5.0 \cdot 10^{-6} \Delta t \cdot (1 + (T_a - T_S))}{\Delta z_1}; \qquad (9)$$

where T_a is an air temperature; T_s is a sea surface temperature; Δz_1 is the thickness of the top layer. The same conservation conditions as for the momentum applies also for the heat. No freshwater source distributed over the sea surface in form of precipitation has been used in the model. The pressure on the top layer is naturally prescribed by the atmospheric measurement data.

The horizontal boundary condition of the Baltic model is the so-called “free radiation” type, meaning that outgoing barotropic waves are unimpeded to leave the model domain. For the salinity, temperature and specific age the exiting scalar properties are instantly lost while water flowing into the model domain assumes the inherently borne scalar property prescribed.

The prescription of the salinity and temperature at the boundary also applies to the ÖG model but the major difference is that the computed and stored sea level elevation data from the Baltic model are prescribed at both of its two (northern and southern) boundaries as well.

The solid vertical walls are prescribed to be no-slip type. Neither these nor the bottom bed are designed to be permeable to the scalar properties except for the locations where the rivers discharge. At these places the salinity is set to zero while the river water instantaneously adapts to the temperature of the ambient water.

The ice dynamics have been formulated in a simple but robust way: at temperatures below 0.2°C the wind stress is lowered a factor 10 and at 0.0°C the heat flux through the ice is shut off as long as cooling condition prevails. The reason for not reducing the wind stress completely is that the wind set-up mechanism by tilting the ice-covered surface remains. It follows that no ice drift mechanism is modelled either.

Finally, there is also a kinematic boundary condition that expresses that a fluid particle on the surface remains on the surface regardless of the advective motion of the underlying layers.

6.3 Numerical features of the 3D-model

The model consists of 18 vertical levels with irregular vertical spacing and with monotonously increasing layer thickness toward the bottom. Depths of layer interfaces are: 0 m, 2.5 m, 7.5 m, 12.5 m, 17.5 m, 22.5 m, 27.5 m, 35.0 m, 45.0 m, 55.0 m, 65.0 m, 75.0 m, 85.0 m, 95.0 m, 105.0 m, 137.5 m, 162.5 m, 187.5 m and bottom. These layers are the same both for the Baltic and ÖG area simulations. An upgrade to a finer vertical resolution would entail a major investment in programming work particularly concerning the graphic presentation program, and has thus not been an option.

A thorough description of the numeric scheme and other model constructs have been given in detail in Sokolov et al. (1997). A brief display of the major model features follows. The finite difference approximation of these equations is constructed by integrating them over the C-grid (*sensu* Mesinger & Arakawa, 1976) cell volume, taking into account the appropriate boundary conditions. A time step is split up as suggested by Liu and Leendertse (1978) for a vertically integrated two-dimensional model. Thus, the u-equations are solved at the time step of n $-1/2$ n $+1/2$ (n denotes a time step number), v-equations are solved at the time step of $n \sim n + 1$, and all other equations are solved at each half time step. All vertical derivatives are treated implicitly. The technique known as mode splitting (Simons, 1974) is implemented. The 2D equation for the volume transport (external mode) is obtained by summation of finite difference approximations of 3D momentum equations over the vertical direction. Before the 3D finite difference equation (internal mode) can be solved, sea surface elevation is calculated from the volume transport equation and a vertically integrated continuity equation.

A bottom frictional stress enters semi-implicitly into both modes and uses a bottom layer velocity to be calculated. This treatment of the bottom friction is realised numerically in

a frame of iterative procedure. That is, the 2D and 3D momentum equations are solved repeatedly until the absolute value of a maximum difference between the bottom velocities at neighbouring iterations becomes less than some small positive number. This adjustment allows using an alternation direction-implicit method for solving the volume transport equation (Liu & Leedertse, 1978; Andrejev & Sokolov, 1989), and to give the same time step as for 2D to the 3D parts of model. The problem is then reduced to three-diagonal algebraic systems and the Gaussian elimination method makes it possible to solve them using standard methods. This scheme allows using a much larger time step than that determined by the Courant-Friedrichs-Levi computational stability condition.

To join these two grids, first all (18) layers of the Baltic Coarse Resolution (CR) grid are interpolated horizontally so as to produce values for the interspersed grid cells of the ÖG area which has a Fine Resolution (FR) grid. If the FR grid is shallower than the CR grid along the boundary, nothing more needs to be done than matching the opposing values on either side of the boundary. If the FR grid is deeper, however, the average value of the four closest neighbouring CR-points is assigned. If these points are also shallower, the layer is assigned the value of the adjacent CR-layer above. After all layers are filled with data, final interpolation to fill in remaining non-assigned values along the FR boundary may be readily performed.

For the simulations of the Baltic and the ÖG area, the same model is thus used but with varied parameters. These are summarised in Table 3.

Table 3. Overview of utilised modelling parameters.

	Baltic modelling	ÖG area modelling
Grid cell size	9261 m	185.2 m
Grid numbers	125×145	133×145
Time step	2 h	3–6 min
Horizontal eddy diffusitity	50 m^2/s	10 m^2/s
Maximal depth	450 m	60 m

6.4 Retention time calculations

The average transit retention time estimates have been computed following Engqvist (1996) and employing eq. (6) for the advective and diffusive transformation of this scalar with the physical dimension of age per unit volume. The added dynamic is the source term that corresponds to the aging, that is, the water contained in the interior of the study area is aged one time step for each time step it remains within the predefined borders. The specific age is naturally set to zero for the water at (and outside of) the boundary, and applies also to the river discharge water. Two parallel retention time computations were performed for the ÖG area: one for the entire area, the other for the BM area. This form of retention time analysis has become an accepted procedure (Mattson, 1996; Gustafsson, 1997).

7 Model results

7.1 Presentation considerations

From a computational point of view, the amount of data produced by this massive simulation effort is impressive, and is also reflected by the demanding task of presenting these data in a fashion that communicates a zest of the intricate and complex dynamics of the processes involved. To give full justice to this numerical endeavour, an animated movie would be required, but this falls outside the scope of this study, however. Therefore it was decided prior to the onset of the simulations that for each state variable we should present the situation at the *initial*, *mid* and *final* stages i.e. 1991-12-31, 1992-06-30 and 1992-12-31. This applies for the fields of salinity, temperature, velocity and sea elevation. Of these four entries, only the last one represents a mere horizontal 2D-distribution, while the other three are fully 3D. In order to substantiate the existence of the vertical dimension, some salinity and temperature distributions over vertical cross-sections have also been added. The scaling of the presented pictures is also problematic. One must choose between the aspect of inter-comparability (i.e. making all scales similar) or the aspect of enhancing particularities of each picture (individually selected scale). A compromise to balance both these aspects was the finally chosen option. The estimates of the retention time together with ensuing statistical analysis – in particular for the BM area – should be the main point of the presentation and will be presented both in tables and diagrams. If not otherwise specifically noted, retention time tacitly refers to the average transit retention time.

7.2 Baltic model results

An initial check of both the Baltic and ÖG models was performed in order to ascertain that the sea level dynamics functioned acceptably. The procedure was the following: First the Baltic model was run for one month of spin-up time with December 1991 atmospheric and other forcing data. Then the computed boundary values and the local part of the same meteorological data plus the local river runoff forcing were permitted to drive the ÖG-area model. The sea level in the corresponding location of the Forsmark harbour was recorded from the simulations on a daily basis so as to facilitate a comparison as closely as possible. The result is given in Fig. 7. It can be seen that basic features coincide acceptably. During the initial phase of this spin-up period the motion of the Baltic waters attains speed from an initial complete standstill. The measured and the simulated sea levels adopt convincingly by the end of the month to approximately the same levels. This favourable result did not motivate any further efforts to check the barotropic model realism. The Baltic model was put into action running one month at a time.

The first results of the Baltic one-year simulation are presented in Fig. 8 and Fig. 9, in which snapshots of the surface distributions of the salinity (Fig. 8) and temperature (Fig. 9) fields are depicted at the beginning (a), midpoint (b) and ending (c) of the study year 1992. The influence of the major river discharges is noticeable as are the heating and cooling effects.

In order to also give a notion of the 3D-depth distribution underneath the surface, the salinity distribution on a cross-section passing through the ÖG area is presented in Fig.10a–c for the same dates as above. The curved isohaline surfaces indicate cross-sectional flows.

The sea level elevation is presented similarly in Fig. 11a–c and the surface current patterns are depicted in Fig. 12a–c. From these pictures the strong influence of wind stress is evident as is the effect of the earth rotation forcing water to the right of the wind.

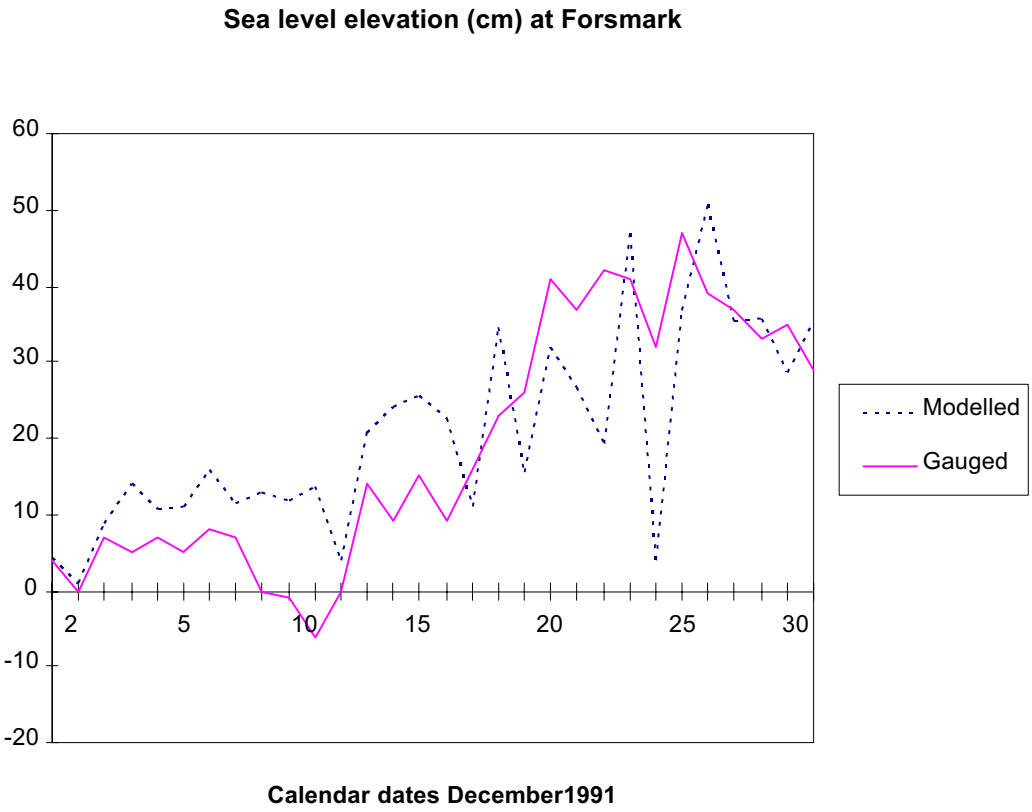

***Figure* 7.** *Comparison between modelled and measured sea level elevation pertaining to Forsmark harbour during the spin-up month December 1991.*

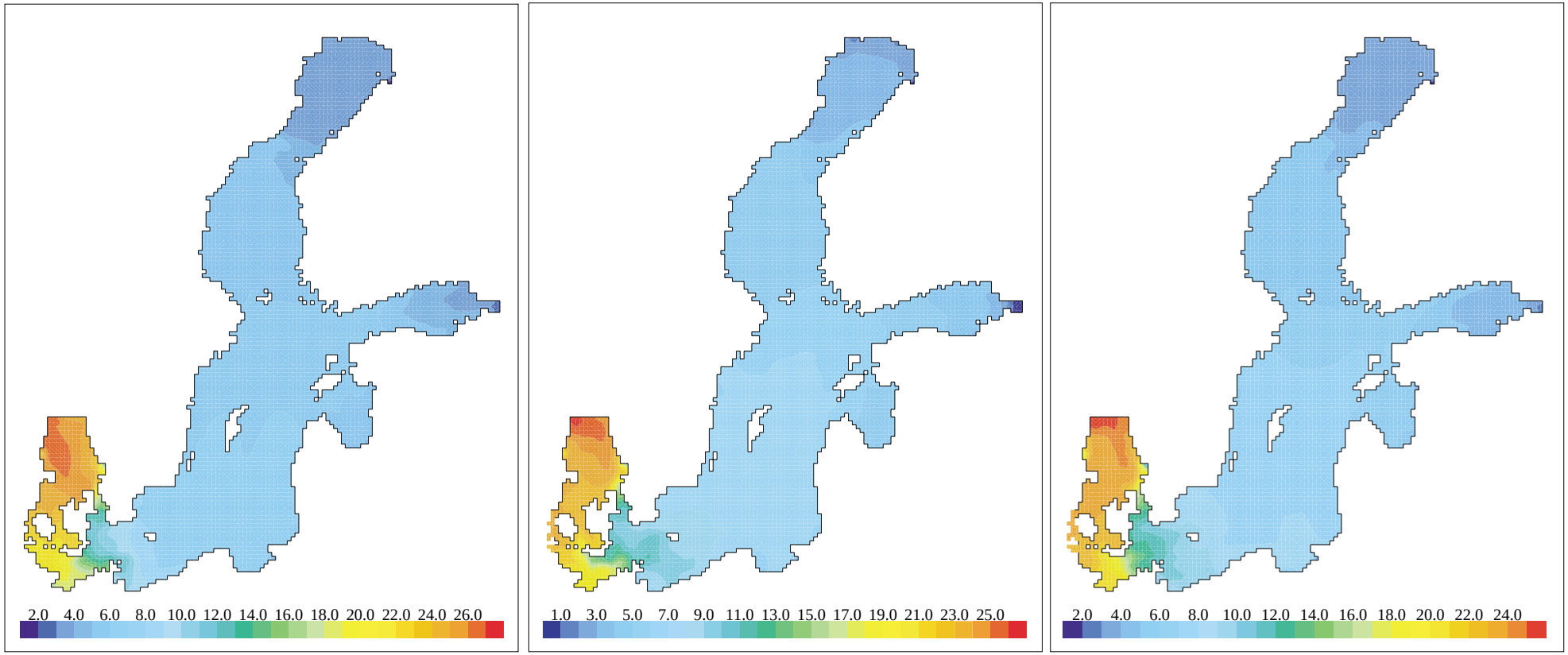

Figure 8 a-c. *Modelled surface salinity distribution of the Baltic model 1992-01-01 (a), 1992-06-30 (b) and 1992-12-31 (c).*

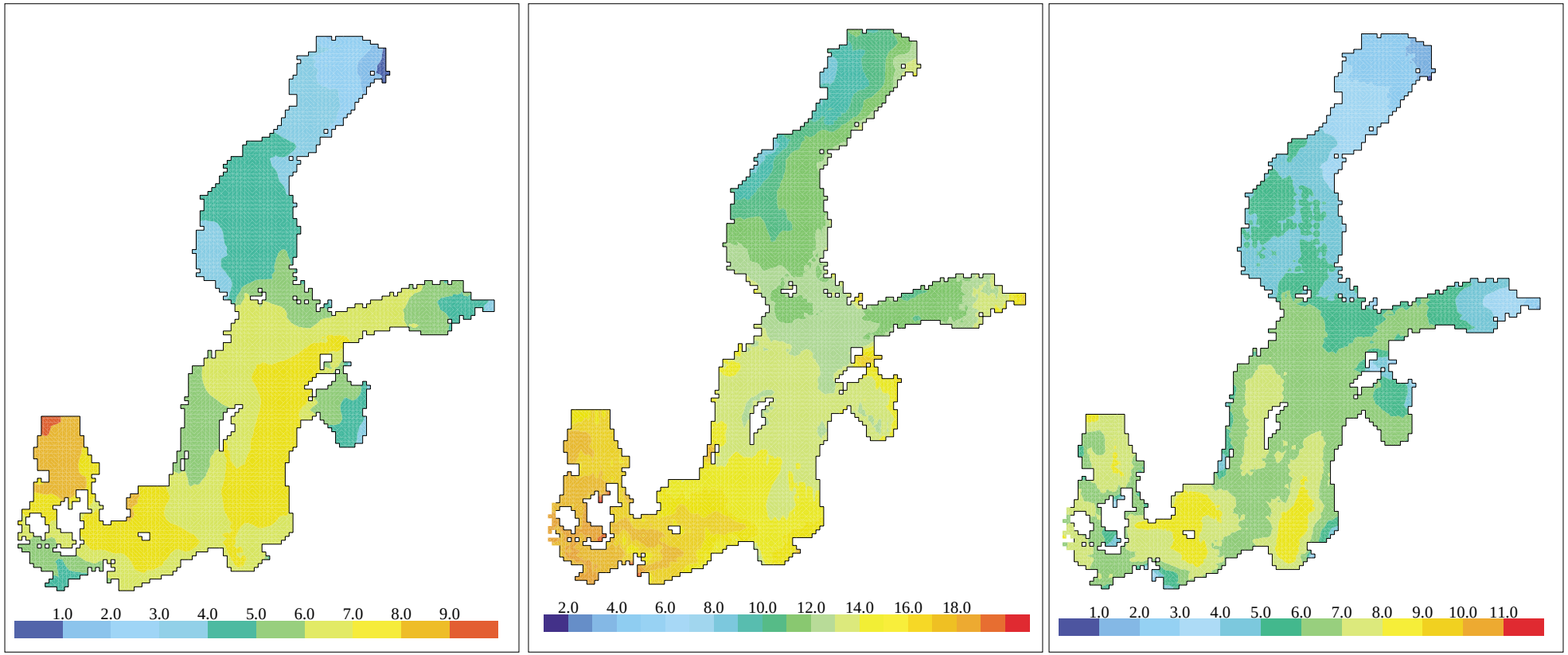

Figure 9a–c. *Modelled surface temperature (ºC) distribution of the Baltic model 1992-01-01 (a), 1992-06-30 (b) and 1992-12-31 (c).*

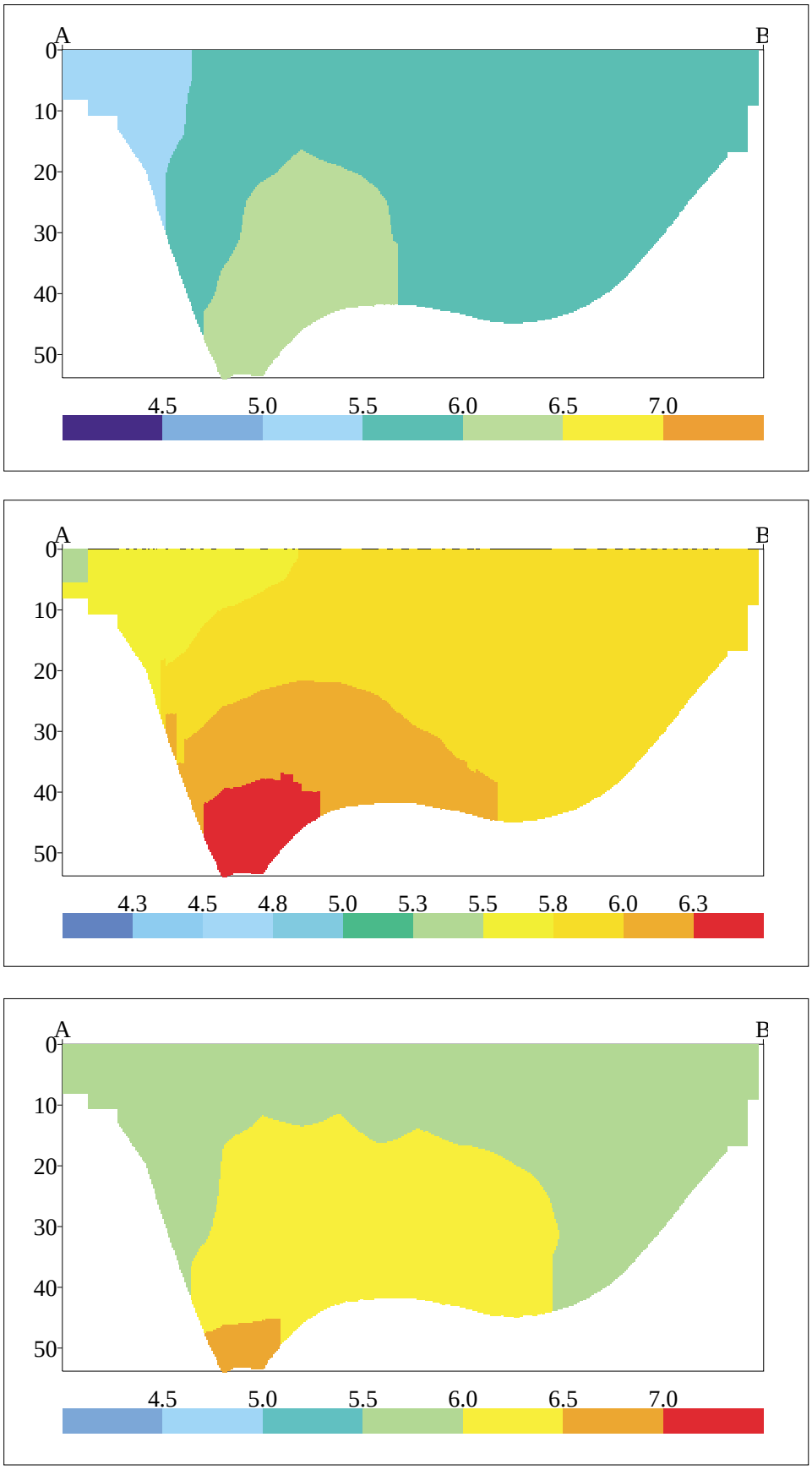

Figure 10a–c. *Modelled vertical salinity distribution in a cross-section 1992-01-01 (a), 1992-06-30 (b) and 1992-12-31 (c). The approximate location of this cross-section is indicated in Fig. 2.*

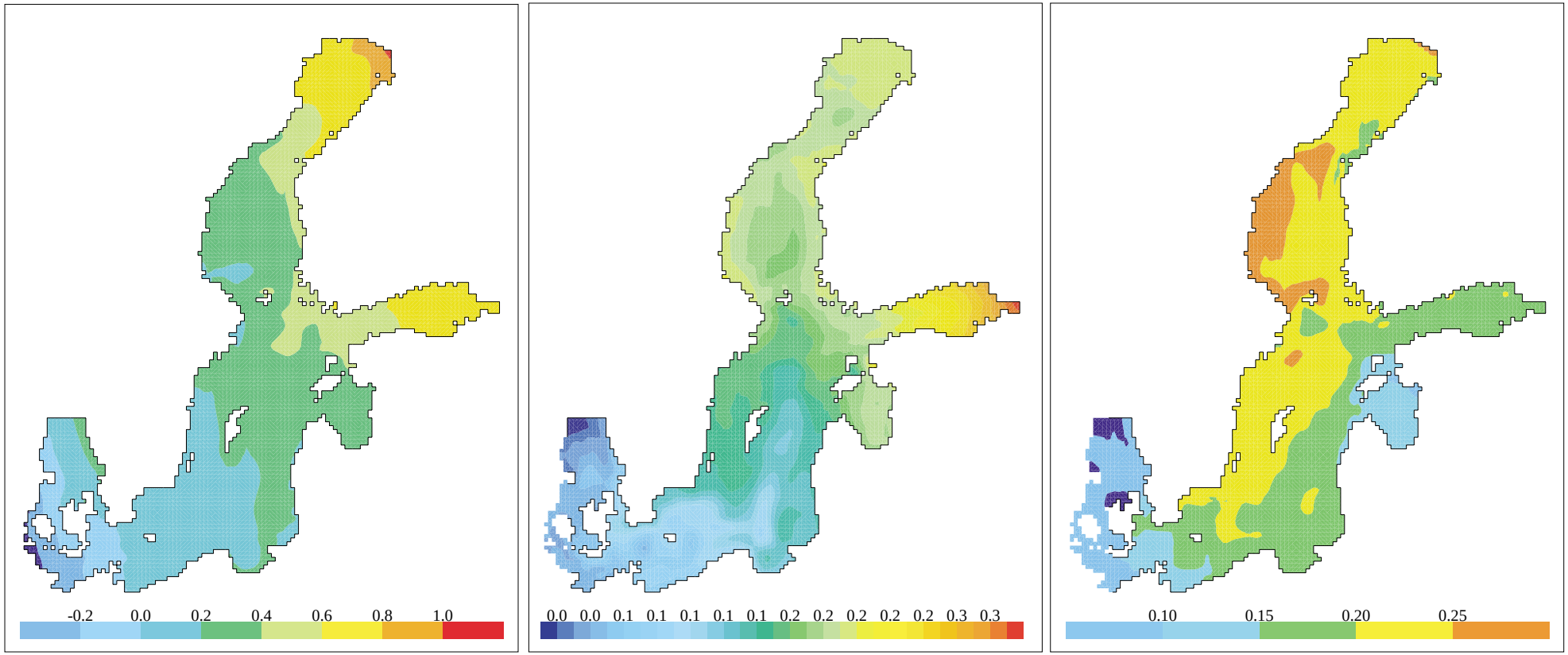

Figure 11a–c. *Sea level elevation (m) of the Baltic 1992-01-01 (a), 1992-06-30 (b) and 1992-12-31 (c).*

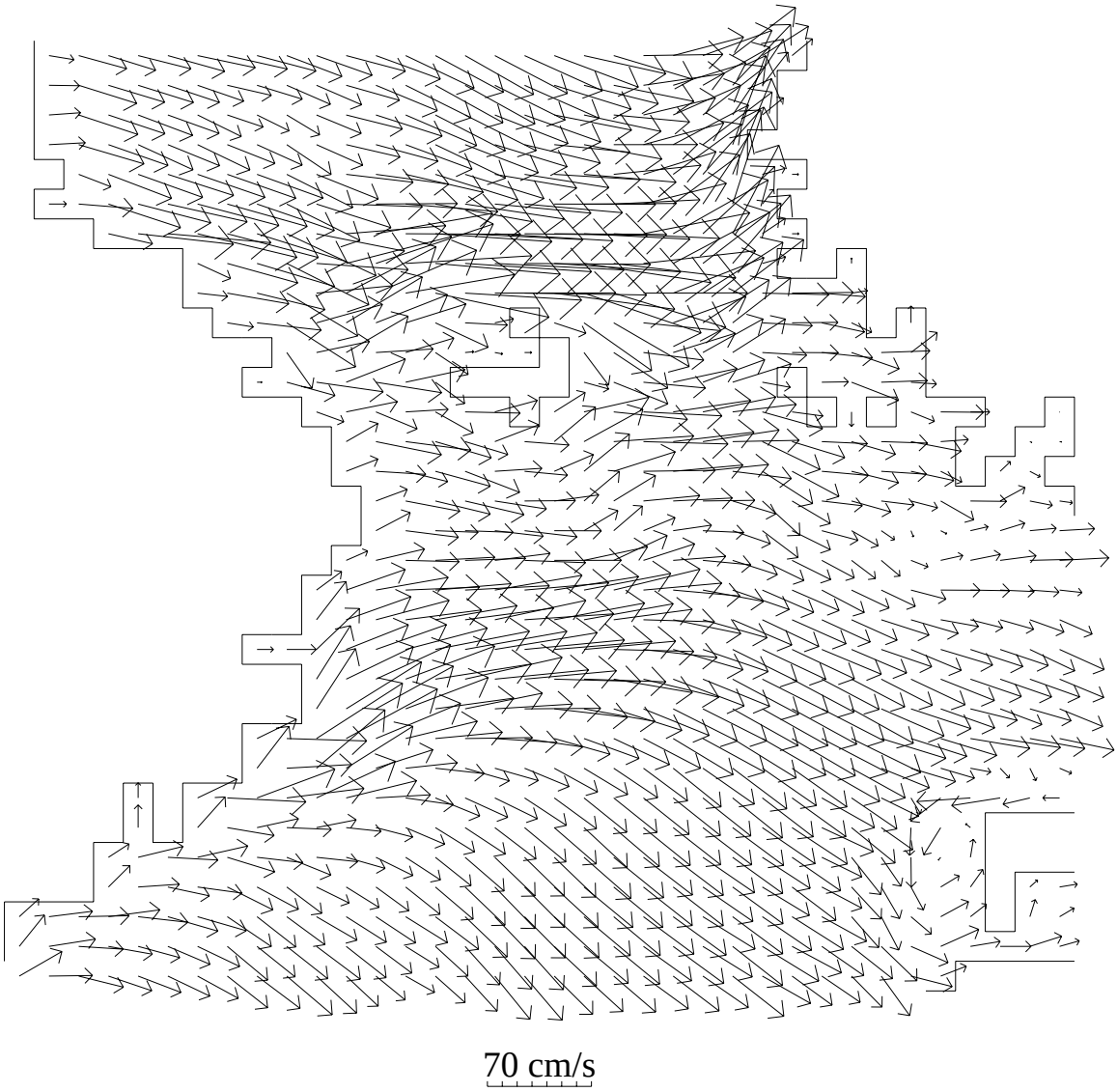

Figure 12a. *Modelled surface velocity distribution of a midsection of the Baltic surrounding the ÖG area on 1992-01-01.*

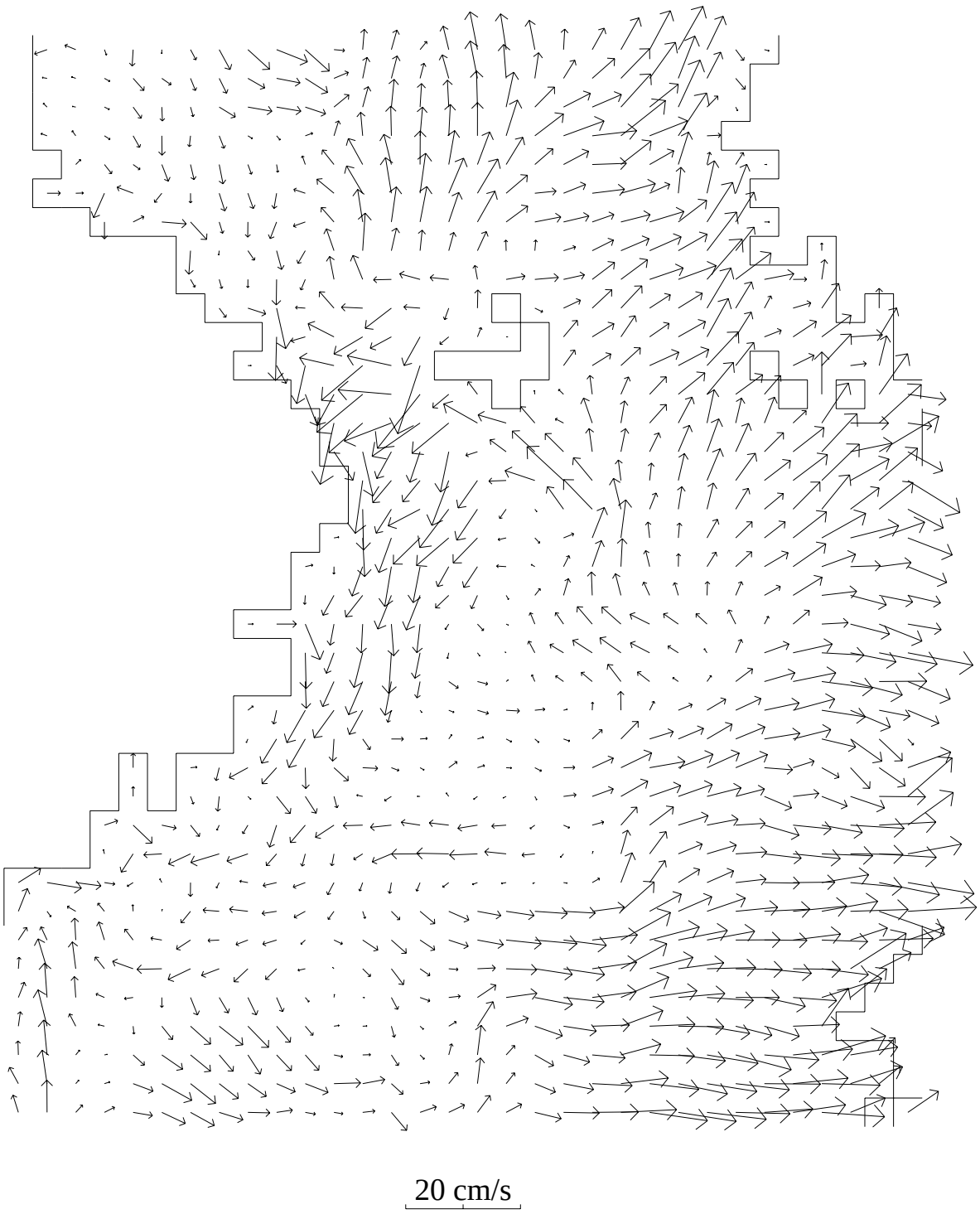

Figure 12b. *Modelled surface velocity distribution of a midsection of the Baltic surrounding the ÖG area on 1992-06-30.*

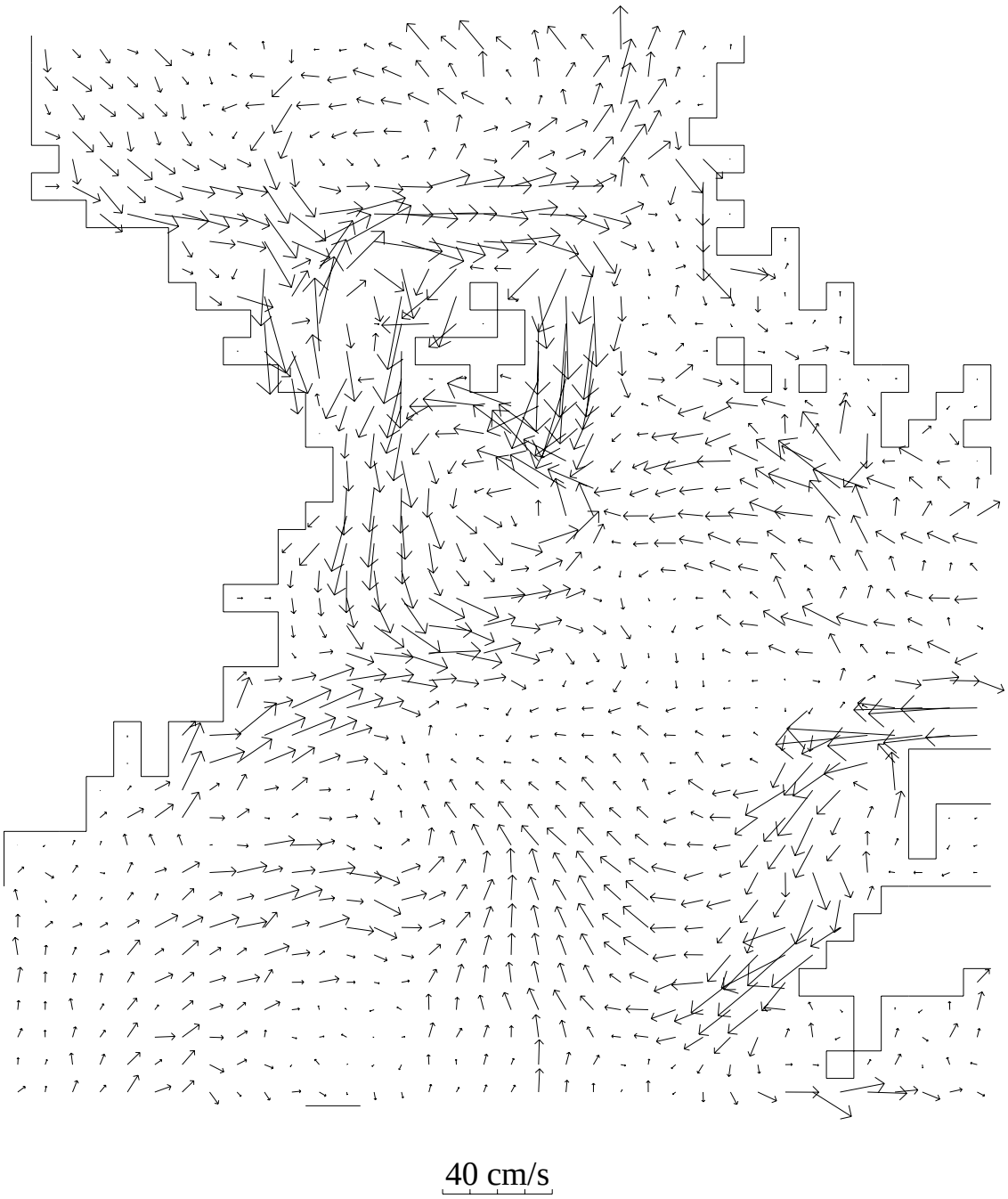

Figure 12c. *Modelled surface velocity distribution of a midsection of the Baltic surrounding the ÖG area on 1992-12-31.*

7.3 Öregrundsgrepen model results

The results of the ÖG area simulations are presented analogously as for the Baltic. In Fig. 13a–c and Fig. 14a–c the surface salinity and temperature distributions are depicted. The salinty depletion at the mouth of the Kallriga bay where the two streams discharge is clearly visible. Except for this the salinity surface distribution is homogeneous. The surface temperature has a comparatively higher degree of variation, most likely because of the faster heating/cooling processes taking place in the shallower area.

There is also a triplet of interesting pictures displaying the surface distribution of the retention time. The first one of these differs from the routine of using the start of the year 1992 as initial data presented. Instead the end of January 1992 is displayed. This is because on January 1, 1992, when the ÖG simulations began, the initial retention time was set to zero. A better procedure would, in retrospect, have been also to allow a spin-up period also for the ÖG area simulations. This oversight casts some doubt on the validity of the retention times estimates of January 1992. Due to the occurrence of several storm events during the beginning of this month that intensely rejuvenated the ÖG waters, it seems plausible that the negative consequences are limited to affect only the initial stage of this month. In Fig. 15a–c the rejuvenation of the surface water either from the northern and southern boundaries or at the mouth of the Kallriga local estuary can be seen, although this latter effect is counteracted by the notable tendency of recirculation. In more secluded coastal areas with no freshwater discharge, the more or less stagnant water is obviously of higher age. The advantage of the present dynamic method to estimate the retention times compared to the morphometric methods put forward by e.g. Perssson et al. (1993) is obvious when viewing the high degree of spatial and temporal variation in Fig. 15a–c.

The cross-sectional pictures Fig. 16 (temperature) and Fig. 17a–c (salinity) show that the vertical gradients are feeble. The thermocline that was built up during June 1992 had all but eroded on the occasion of the snapshot presented in Fig. 16.

The sea level elevation (Fig. 18a–c) is displayed mostly as a longitudinal distribution. During a northerly storm event on 1992-07-28 (see Fig. 6) a deviating pattern occurs indicating a gyre in the northern part of the ÖG area. A similar situation is shown in Fig. 18a and the corresponding velocity field is depicted in Fig. 19a. In all of the velocity rendering pictures (Fig. 19a–c), the subtle effects (Csanady, 1982) of the underwater topography may be clearly seen.

The trailing analysis of the retention time is presented in Table 4 and graphically in Fig. 20. One sees a rising retention time for all layers that culminates in summer, declining and stabilising on an approximately equal level for all layers by the end of the year. A closer look reveals, as has been epitomised in Fig. 21, that the average retention time does not monotonously increase with depth but has a minimum for the layer centred around 40 m of depth. The likely explanation is that the baroclinically driven intermediary exchange expresses itself by renewing the bottom water above the deeper isolated bottom trenches and holes.

Table 4. Monthly averages of the retention time (days) of ÖG area with regard to depth. The (grand) yearly averages are also presented.

	Depth of layer midpoint (m)									
	1	**5**	**10**	**15**	**20**	**25**	**34**	**40**	**50**	**60**
Jan	2.0	2.1	2.0	2.1	2.5	3.1	3.3	3.2	4.9	9.6
Feb	3.7	3.8	3.7	3.8	4.4	5.6	5.8	5.7	9.1	12.5
Mar	6.0	6.0	5.9	6.1	6.5	7.7	7.5	6.7	12.0	19.6
Apr	9.0	8.8	8.0	7.6	7.8	8.7	7.6	5.6	10.3	23.3
May	10.9	10.7	9.9	9.1	8.5	8.7	7.3	5.4	15.5	24.5
Jun	16.2	16.1	15.5	15.8	17.2	19.6	18.1	14.8	35.0	40.4
Aug	13.2	13.0	12.3	11.5	10.6	10.6	8.5	5.6	22.1	42.2
Sep	17.3	17.2	16.3	15.8	16.1	17.6	15.3	11.0	19.2	33.8
Oct	19.0	19.0	18.1	17.2	17.3	19.1	17.1	13.4	23.2	36.5
Nov	17.8	17.6	16.7	15.9	15.5	16.8	14.7	11.0	19.0	19.6
Dec	17.6	17.6	17.4	17.3	17.4	18.9	16.5	12.5	21.5	21.9
Avg.	12.1	12.0	11.4	11.1	11.2	12.4	11.1	8.6	17.4	25.8

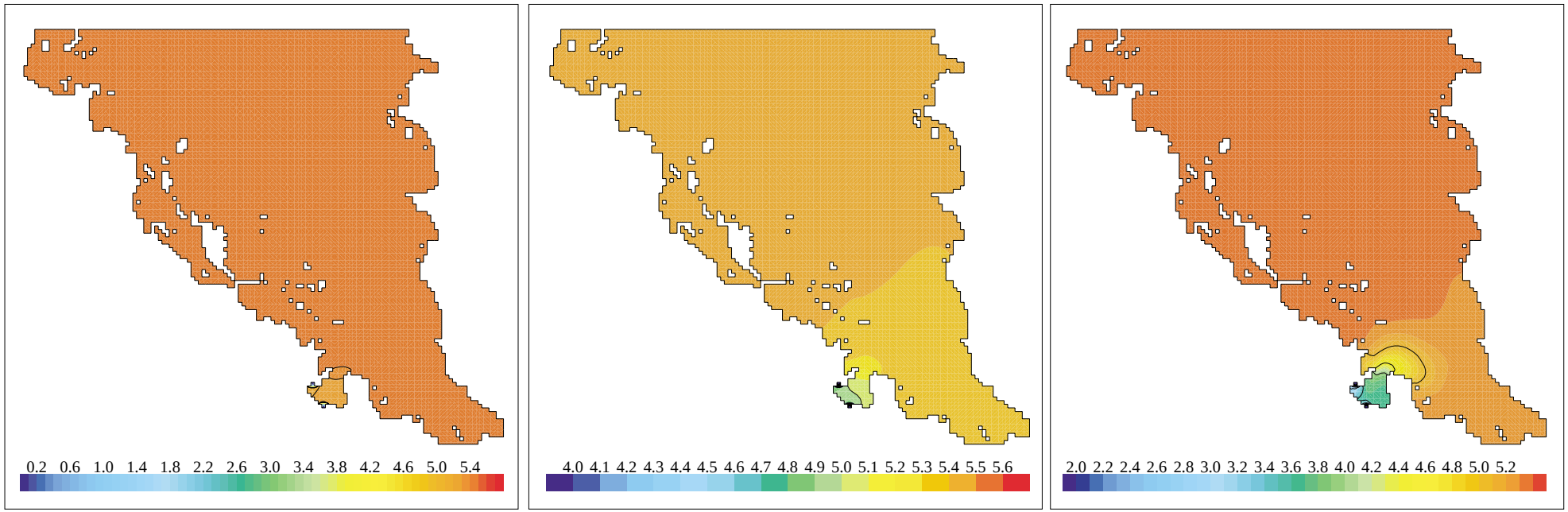

Figure 13a–c. *Modelled surface salinity distribution of the ÖG area model 1992-01-01 (a), 1992-06-30 (b) and 1992-12-31 (c).*

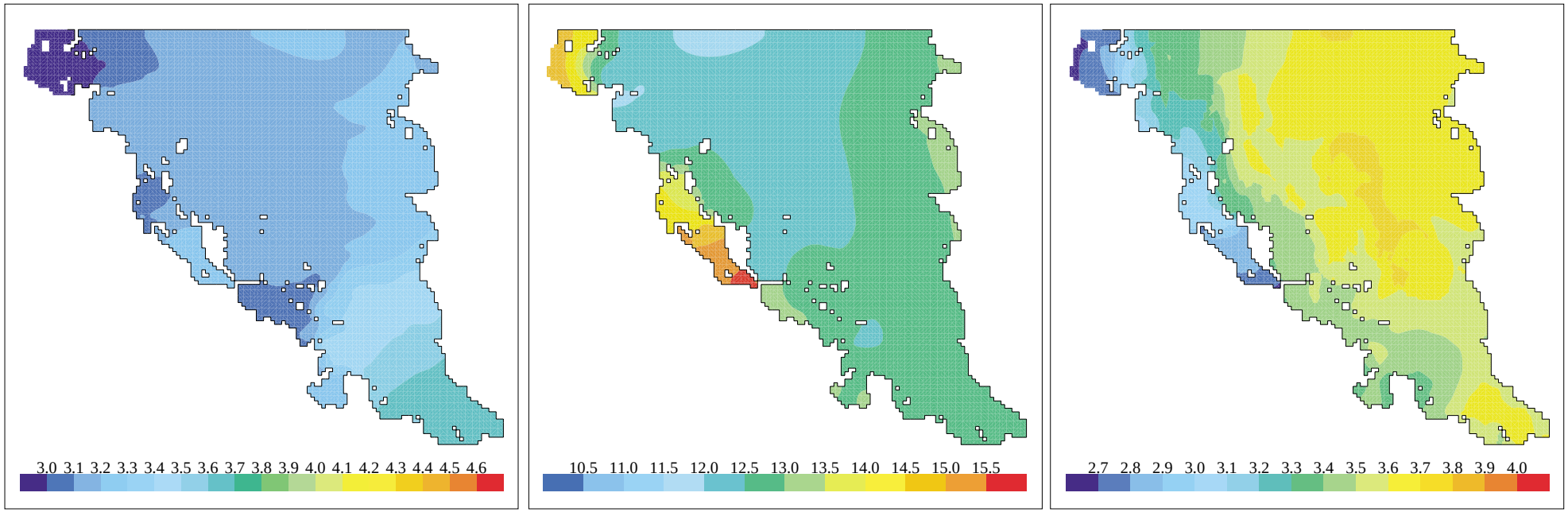

Figure 14a–c. *Modelled surface temperature (° C) distribution of the ÖG area, 1992-01-01 (a), 1992-06-30 (b) and 1992-12-31 (c). Note the rapid heating of the water of the shallow areas closer to the coast in the summer (b).*

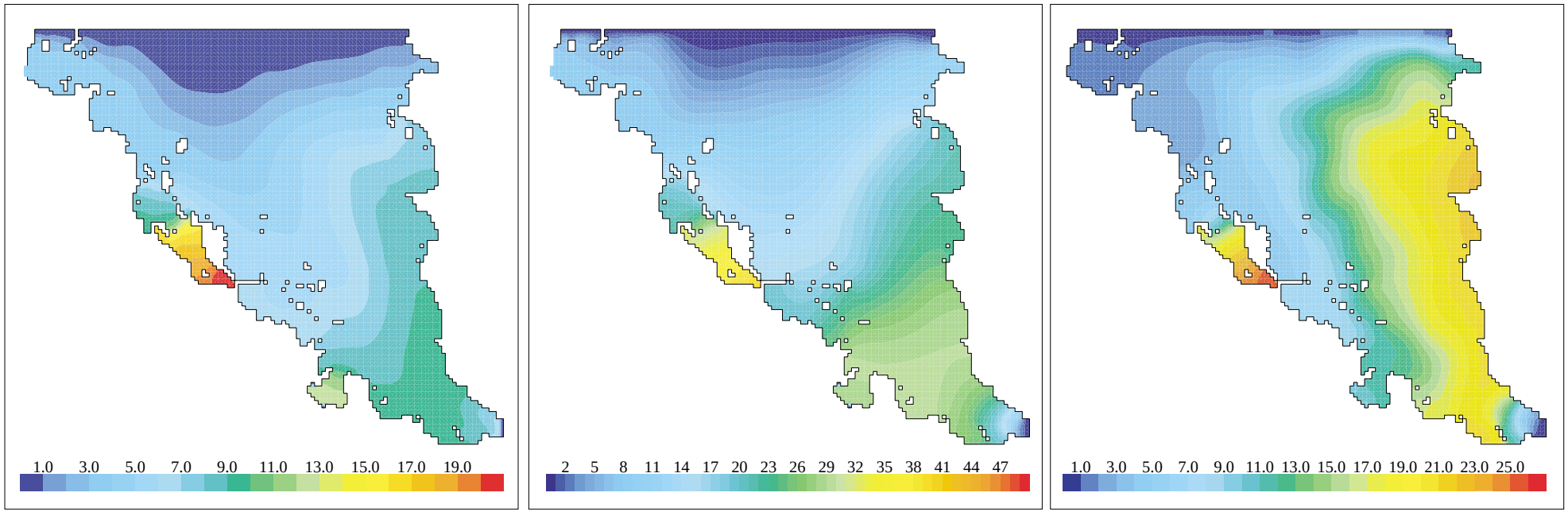

Figure 15a–c. *Modelled transit retention time (days) distribution of the ÖG area, 1992-01-31 (a), 1992-06-30 (b) and 1992-12-31 (c). The initial date deviates from the routinely chosen January 1, 1992, by being delayed one month. The reason is that the initial retention time was set to zero and one month of spin-up must be allowed to attain a non-trivial quasi-stationary equilibrium. The oldest water is found in the secluded coastal creeks and the rejuvenating exogenous water enters through the north and south boundaries.*

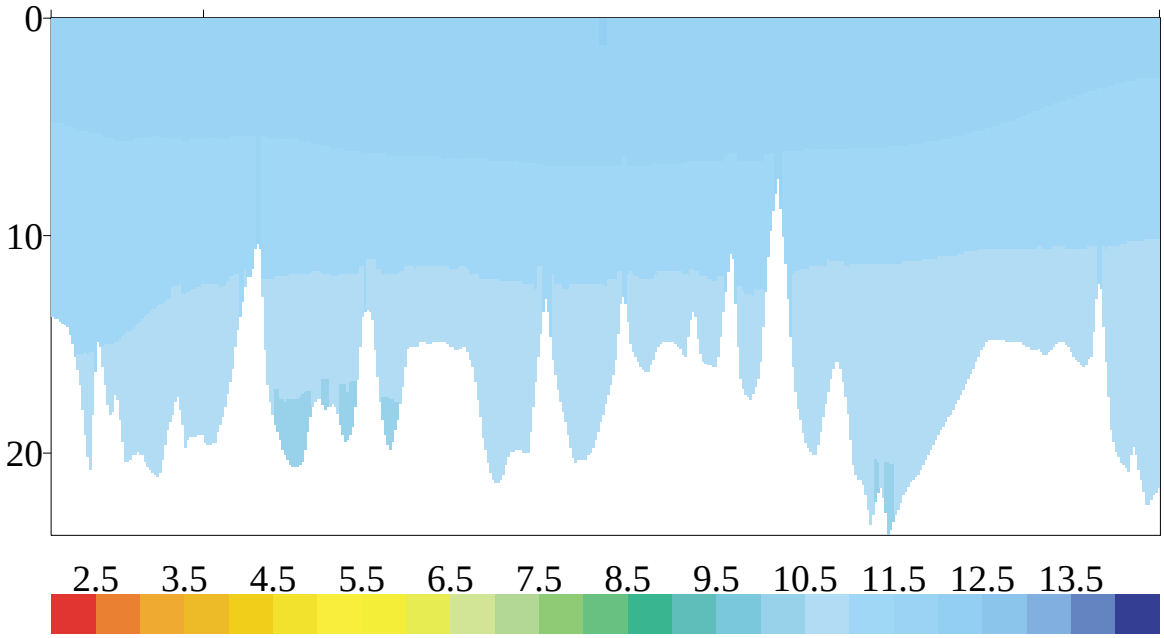

Figure 16. *Modelled vertical temperature (ºC) distribution in a cissect along the bay axis of the ÖG area 1992-06-30. The location of this cross-section is indicated in Fig. 3. The build-up of the summer stratification is in progress but strong winds prior to the depicted date diminished the vertical thermal gradient. At the beginning and ending of the simulation year the thermal stratification situations were even more feeble and are therefore not presented.*

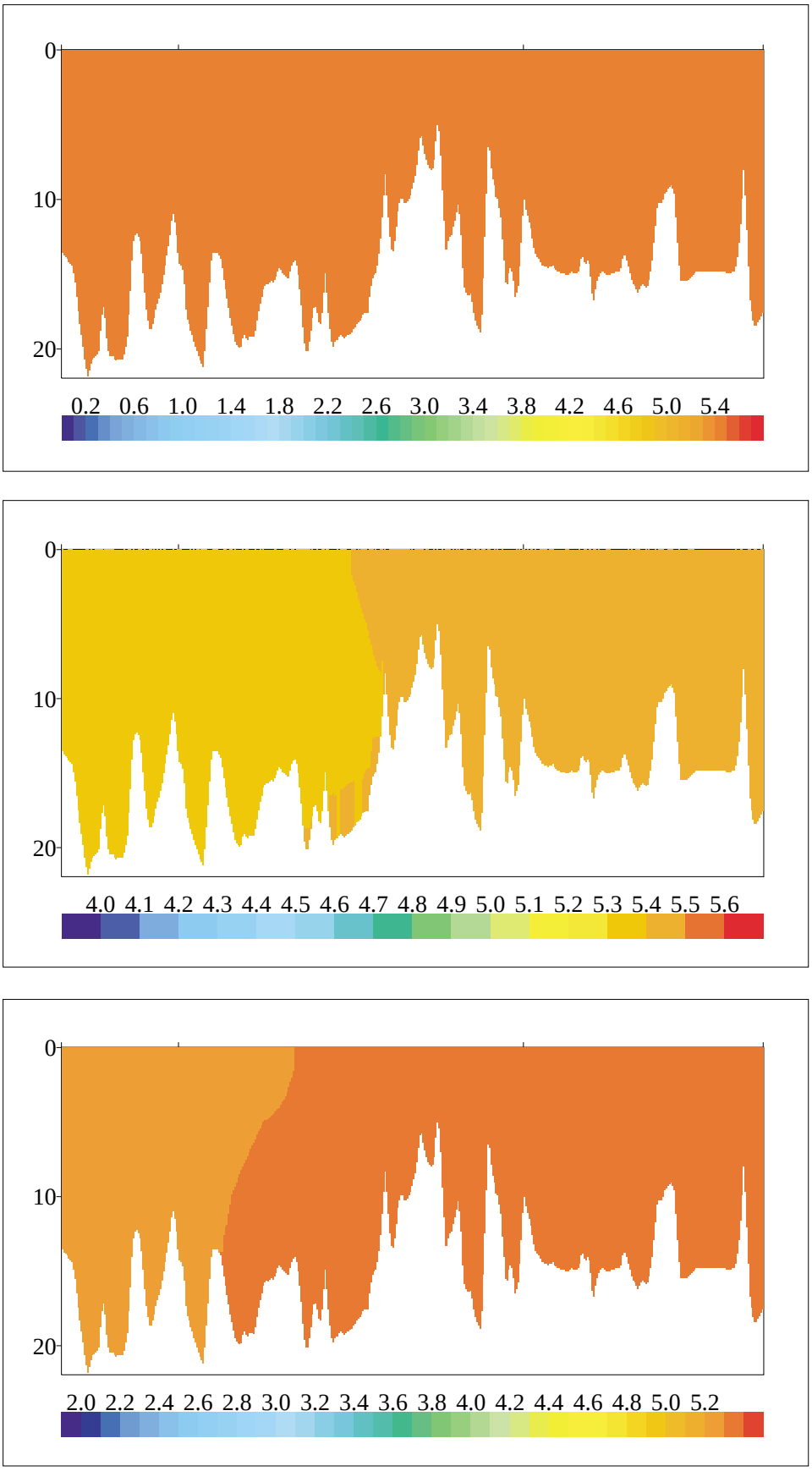

Figure 17a–c. *Modelled vertical salinity distribution in a cross-section (see Fig. 3) near the ÖG area 1991-12-31 (a), 1992-06-30 (b) and 1992-12-31 (c). All these snapshots display rather homogeneous salinity conditions. In (a) the vertical stratification is next to complete due to mixing induced by strong wind.*

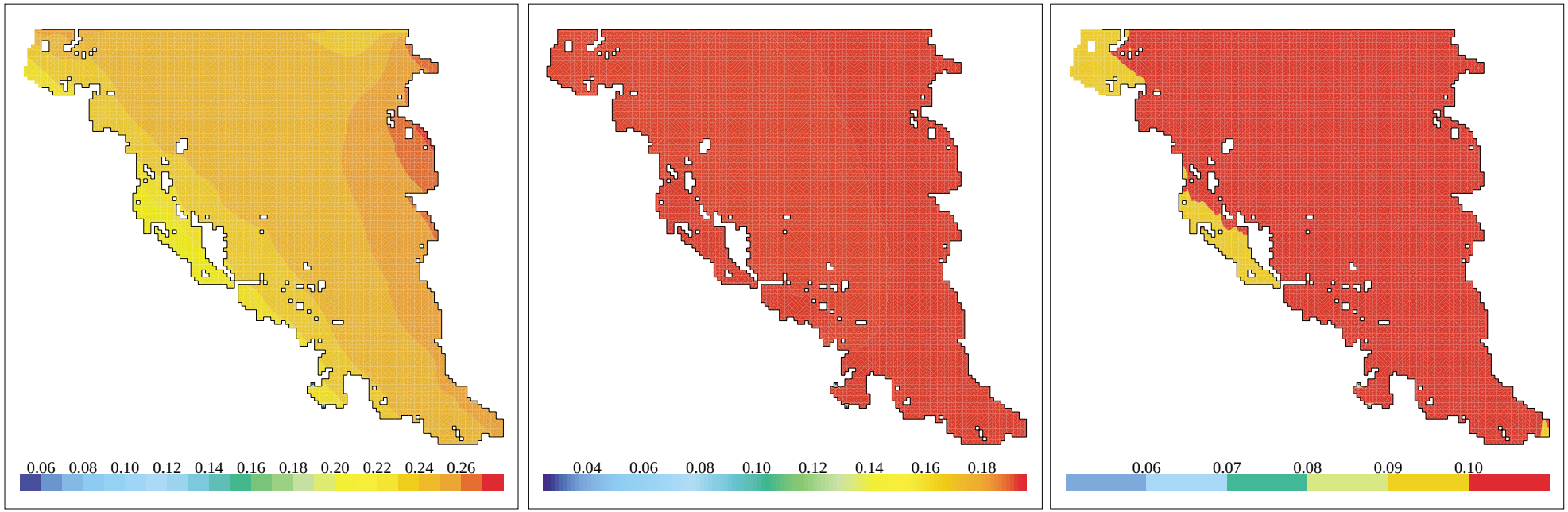

Figure 18a–c. *Sea level elevation (m) in the ÖG area 1992-01-01 (a), 1992-06-30 (b) and 1992-12-31 (c). The sea level variability is mainly a reflection of the local wind forcing which was quite feeble in (b).*

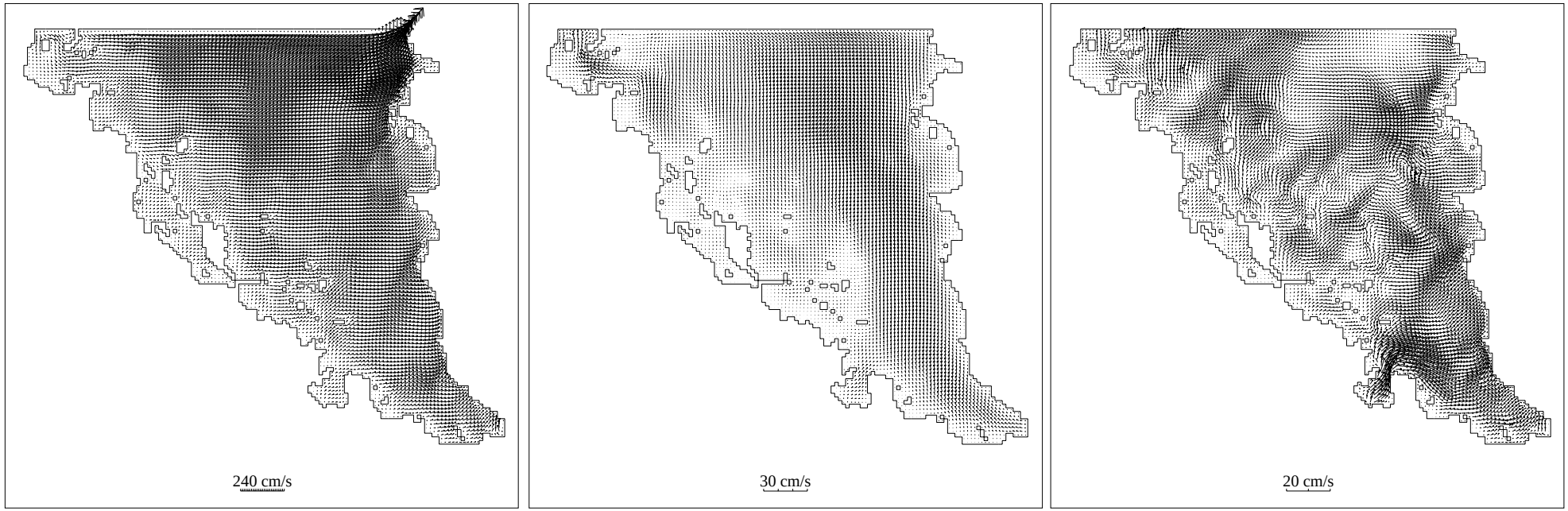

***Figure 19a–c**. Modelled surface velocity distribution of a midsection of the Baltic surrounding the ÖG area on 1992-01-01 (a), 1992-06-30 (b) and 1992-12-31 (c). Note the strongly compressed scale in (a), indicating intense surface velocities.*

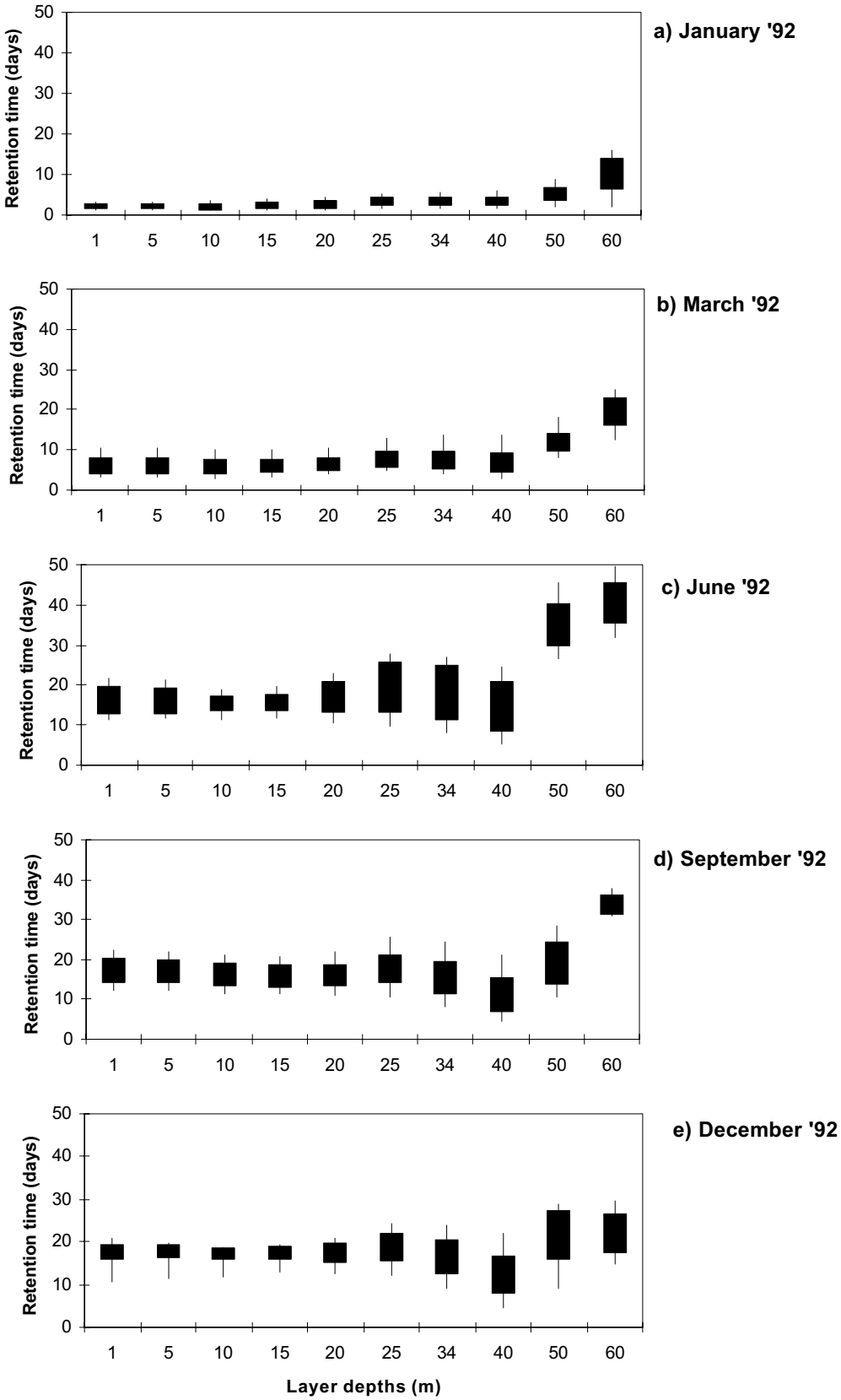

Figure 20a–e. *Statistical properties for the ÖG area depicting the variation range of the average retention time with regard to the mid depth of the respective layers. The variation is expressed as a thin line connecting the maximum and minimum values which is intersected by a broader line displaying ± 1 S.D. (standard deviation) relative to the monthly average. These statistics are based on a temporal resolution of 0.5 hour, i.e. the data are read out in a pace that varies between every 5th to every 10th time step.*

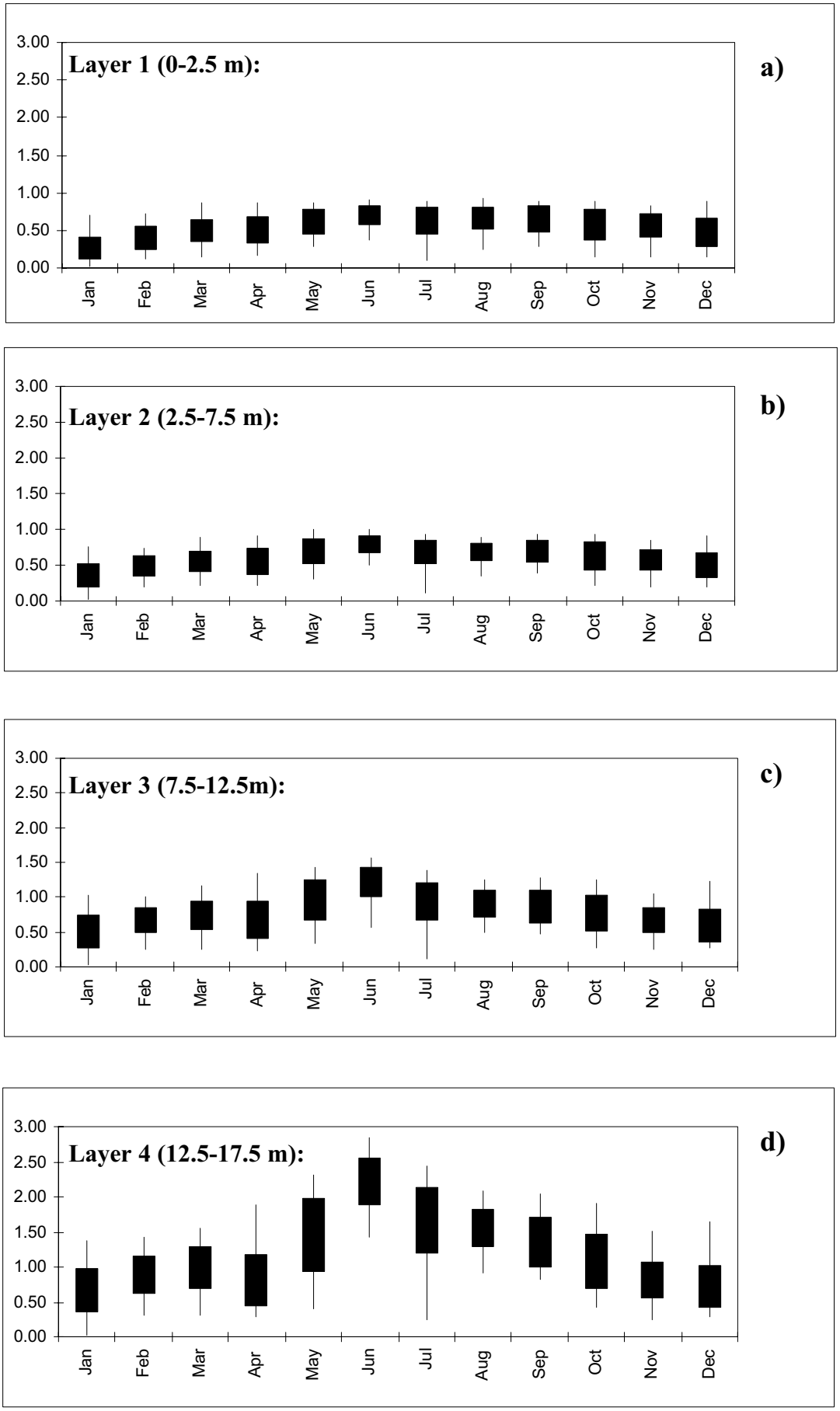

Figure 21a–d. *Variation range of the average retention time for the four layers of the BM area. The variation is expressed as a thin line connecting the maximum and minimum values and is intersected by a broader line displaying ± 1 S.D. (standard deviation) relative to the monthly average. These statistics are based on a sampled temporal resolution of 0.5 hour.*

7.4 Biomodel area ventilation results

The average retention times for each of the four layers of the BM area are listed in Table 5. As for the entire ÖG area the retention times increases towards the bottom and peaks at the month of June. The average retention time over the entire BM area is also computed taking into account the volume of the respective layers (see Table 2). From Table 6, where the corresponding volume flows passing through the layers are tabulated, the column representing the total flow passing through the BM area is adjoined to Table 5. The quotient between the total volume of the BM area and these total volume fluxes give another estimate of the retention time, which may be called *well-mixed retention time*, which would coincide with the average transit retention time if a steady-state flow through a well-mixed basin were arranged. Half of this measure would be the resulting retention time if an orderly and non-mixed flow of the same intensity, a so-called *plug flow*, were to be led through a pipe-like basin with the same volume as the well-mixed aforementioned one. Dividing the nominal BM volume with twice the amount of the modelled total flow thus yields the *plug-flow retention time* which cannot exceed the average transit retention time from the simulations. Reassuringly, all monthly values comply. For a well-mixed flow the ratio between the average retention time and the plug-flow retention time would be, as inferred above, a factor 2. The actual ratio varies between 1.02 (June) and 2.34 (January), with an average of 1.81, meaning that the flow-through may be loosely characterised as almost well-mixed. An unevenly partitioned flow, and particularly if it is unsteady as well, could theoretically attain an infinite retention time. An isolated water parcel confined indefinitely (e.g. in a bottom cavity), ages infinitely. Likewise, a substantial intensification of one single peak flow event (out of several distributed over a given time period) will not lower the average retention time very much, since this measure would already be low and the duration of the increased flow short. The plug flow retention time will on the contrary be considerably lowered in direct proportion to how the extra flow compares to total flow over the entire time period. Therefore there cannot exist any generally valid exact relationship between the bulk through-flow and the average retention times.

Table 5. Monthly resolved retention time (days) of BM area with regard to depth and the average volume flow (m^3/s) across the model border.

	Layer 1	Layer 2	Layer 3	Layer 4	Volume average	Vol. flow	PlugFlow ret. time	Ratio (Vol. avg./ Plug Flow)
	(days)	(days)	(days)	(days)	(days)	(m3/s)	(days)	
Jan	0.266	0.355	0.507	0.666	0.447	4659	0.191	2.34
Feb	0.400	0.484	0.666	0.882	0.605	2605	0.342	1.77
Mar	0.496	0.552	0.731	0.993	0.688	2035	0.437	1.57
Apr	0.512	0.556	0.672	0.809	0.635	2414	0.369	1.72
May	0.620	0.691	0.965	1.461	0.924	1350	0.659	1.40
Jun	0.699	0.791	1.216	2.221	1.212	751	1.185	1.02
Jul	0.629	0.683	0.936	1.660	0.964	1626	0.547	1.76
Aug	0.656	0.684	0.905	1.556	0.937	1241	0.717	1.31
Sep	0.650	0.693	0.858	1.359	0.881	1389	0.641	1.38
Oct	0.574	0.631	0.771	1.080	0.759	1827	0.487	1.56
Nov	0.564	0.581	0.669	0.812	0.653	2180	0.408	1.60
Dec	0.472	0.498	0.592	0.712	0.566	2950	0.302	1.88
Avg.	0.545	0.600	0.791	1.184	0.773	2086	0.427	1.81
S.D.	0.124	0.119	0.195	0.472	0.215	1025	0.260	0.331
%	23	20	25	40	28	49	61	18

In Fig. 21a–d, finally, variation ranges of the BM area average transit retention times for the four layers are depicted showing the maximum, two standard deviations, S.D., (counted ± from the average) and the minimum values for the respective months. Again it is seen that the retention time increases toward the bottom and has a marked peak for the summer months when the thermal stratification produces buoyancy forces that counteract vertical mixing.

Table 6. Monthly resolved volume fluxes (m^3/s) entering and exiting through the BM area boundary. The flows are subdivided into the four layers that constitute the modelled BM area. The sum of the entering and the sum of the exiting flows differ slightly due to the difference in sea level elevation between the beginning and end of the month.

Month	Entering flows (m^3/s)					Exiting flows (m^3/s)				
(1992)	Layer 1	Layer 2	Layer 3	Layer 4	Pos. sum	Layer 1	Layer 2	Layer 3	Layer 4	Neg. sum
Jan	2984.2	1499.6	165.7	9.4	4658.8	−2410.1	−1425.9	−735.4	−85.8	−4657.2
Feb	1694.3	736.5	162.2	11.6	2604.7	−1356.9	− 753.2	−450.9	−42.8	−2603.8
Mar	1138.6	622.9	253.4	20.2	2035.0	−1258.3	− 472.6	−277.9	−25.3	−2034.1
Apr	1398.1	660.1	326.2	29.6	2414.0	−1163.6	− 825.3	−395.7	−29.3	−2413.9
May	680.8	460.6	195.5	13.2	1350.1	− 861.6	− 286.0	−187.5	−15.0	−1350.2
Jun	447.4	224.1	74.5	5.2	751.2	− 424.5	− 223.2	− 95.3	− 7.6	− 750.6
Jul	922.2	523.8	166.7	13.4	1626.1	− 863.2	− 469.4	−269.7	−23.0	−1625.2
Aug	631.4	422.6	175.5	11.5	1241.0	− 807.9	− 252.5	−166.7	−13.8	−1240.9
Sep	904.4	335.1	137.3	12.4	1389.2	− 663.4	− 414.7	−286.1	−24.5	−1388.7
Oct	1298.9	349.9	161.5	16.9	1827.2	− 843.6	− 605.5	−348.2	−29.1	−1826.4
Nov	1235.1	576.1	336.0	32.5	2179.6	−1301.0	− 519.6	−329.2	−29.5	−2179.3
Dec	1626.2	924.3	378.0	22.0	2950.4	−1870.9	− 562.8	−464.9	−51.5	−2950.1

The inter-monthly variation of the transit time for the entire BM area amounts to 0.220 days, or 29% of the average value (0.77 days) according to the bottom line of Table 5. The average S.D. for the intra-monthly variations amounts to 0.218 days, which is thus in parity with inter-monthly variation.

It would be interesting to perform a sensitivity analysis by a systematic variation of the forcing factors. Because of the massive computation demanded just to complete one year cycle with the nominal parameter settings, this must be postponed or replaced by possible future simulations with altered ambient conditions such as a considerably lowered sea level, anticipating the long-term consequences of the ongoing landrise.

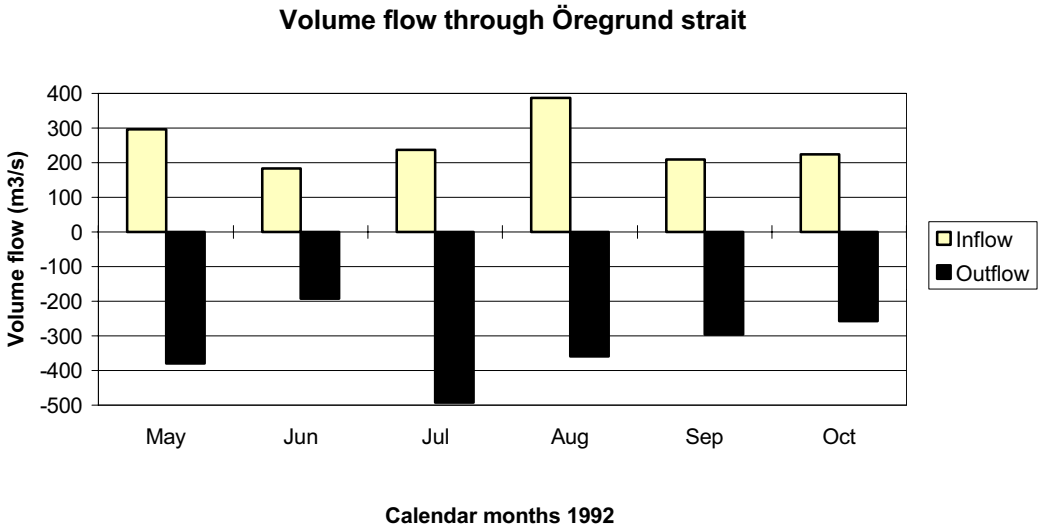

Figure 22. *Volume flow through the southern strait of the ÖG area near Öregrund. The nature of these flows is believed to be mainly barotropic, i.e. the opposing flows mostly occur separately in time. The inflow corresponds to a current setting in the north direction. It is clear that the south-going currents dominate and that the average intensity is somewhat less than that Person et al. (1993) states, namely a mean flux of 540 m^3/s. This statement is, however, given without any context.*

8 Discussion

Numerical models are not and cannot reflect the entire reality, but they represent an aspect of the dominating processes expressed as mathematical equations, permitting them to interact simultaneously. There must thus exist a trade-off between the realism, the accuracy and the generality for any model, numerical or not (e.g. Patten, 1968), when evaluating its capacity to simulate an almost infinitely intricate reality. It is believed, however, that the present effort to achieve the water exchange of the ÖG area represents the state of the art. The entire set-up of this study is certainly a striking example that the lack of measurement data may be compensated by more computing. The sole purpose of Baltic simulations has been to compensate for the absence of relevant and sufficiently frequent forcing data in the vicinity of the ÖG area. Now that the model has met the challenge of completing a full-year cycle, we feel confident enough to discuss its strengths and shortcomings.

8.1 The realism of the Baltic model

Since the forcing with one exception (meteorological forcing) is concocted from statistical average data, there is little point in validating the result against measurement data. This is underscored by the fact that the initial salinity and temperature fields had to be reassembled from winter month averages spanning three months. The comparison of modelled and measured sea level elevation in Fig. 7 also adds credibility both to the realism and the precision of the barotropic part of the Baltic model formulation.

8.2 Evaluation of the Öregrundsgrepen model

The crucial point of the ÖG area simulation is how well the northern open boundary has been modelled. It seems that the construction of this wide interface is well conceived since the boundary permits opposing flows (Fig. 19a–c) which must be expected as the width is wider than the actual Rossby radius. The sea level validation in Fig. 7 is also reassuring. There are more possibilities for validation of the salinity and temperature fields that were measured 1992 but lack of time has diverted us from completing this. The actual absolute salinity and temperature distributions are somewhat beside the point, however. More important are the spatial gradients responsible for the baroclinically induced circulation. If the absolute salinity and temperatures were to be reproduced as closely as possible, one would feel tempted to resort to a part of the available measurements that are available for data-assimilation and use the remaining data for validation.

The organisation of the atmospheric data in monthly subsets has determined these simulations to be run one month at a time. In spite of an ambition to run all months with identical parameters, this has not been possible, mainly because of the occurrences of elevated wind speeds. For such events the first action taken was to reduce the time step from 6 to 3 minutes, thereby maintaining full continuity of the computed scalar fields but losing information of the time derivatives. If the numerical instability prevailed, the next action would be to increase the vertical diffusivity parameter, K_v, in order to enhance the vertical transfer of the excessively induced horizontal momentum. If the instabilities still were not overcome, parameters pertaining to the vertical heat flux

would also be temporarily altered. This has been the case during the run of April, July, October, November and December 1992.

The presently estimated average retention times for the ÖG area correspond acceptably well to the estimates of Engqvist (1999) who with a less sophisticated approach in the form of a hydraulically coupled two-basin model with 50 layers achieved retention times that as a yearly average spanned 7 to 42 days from surface to bottom. The corresponding values of the present study are 12 and 26 days respectively. The size of the respective modelled areas and the forcing differed, however, so that no difficulty in resolving conflicting data need arise. A special study of the volume flux through the strait of Öregrund (Fig. 22) shows that it falls somewhat less than 540 m^3/s (Persson et al., 1993), a datum that is not set in any context, however.

A surprising means of checking the model result of the ÖG area stems from current measurements of Lindell and Kvarnäs (1978). They found a maximum in their current measurement at depths of 35–40 m. This finding corresponds exactly with the found dip in the retention time at the same depth range in the present model (Fig. 20c–e). Even if this coincidence is not conclusive, it must be regarded as strongly corroborative.

8.3 The biomodel area ventilation

To the present authors' knowledge there has not been any attempt made to actually measure the water turnover of the BM-area. The box-model approaches (e.g. Sundblad et al., 1983) do not involve sub-basins that even remotely resemble the BM-area. The possibilities for cross-checking the present results therefore seem exhausted. There was, however, a first coarse estimate of the BM retention time performed by one of the present authors in May 1998. The model approach followed Engqvist (1999), but with an added coupled basin with the approximate dimensions of the present BM area. A correction for the local average wind was applied. These pairs of yearly averages are presented in Table 8. For the bottom water the coarser estimate exaggerates the retention time but for the surface water it seems acceptable.

Table 8. Comparison between two different estimates of the BM area retention time.

	Retention time (days)	
	Present model	**Coarse estimate**
Layer 1	0.55	0.45
Layer 2	0.60	0.70
Layer 3	0.79	3.0
Layer 4	1.2	8.0

9 Conclusions

The present estimation of the water exchange of both the ÖG and the BM areas seems to acceptably fulfil objective criteria of similarity with observed manifestations of the circulation on the instances that permit checking.

A marked inter-monthly variability is displayed in both the retention time of the BM area and even more so by the through flow of its boundary. In spite of the occurrence of severe storms, the present model approach has been proven to be sufficiently robust from a numerical point of view to handle even such extreme forcing episodes, when allowing for reasonable changes of the parameter set-up.

The conclusion must follow that a modelling method has been achieved for computing the circulation of coastal embayments that makes it possible to extend its domain of operation into circulation modes that are driven by even radically altered forcing. The reliance on basic hydrodynamical laws and dependence mainly to accessible large-scale forcing, certifies a general validity. As long as the cascaded pair of models are permitted to operate in parameter spaces that are similar to the ones presently used, inter-comparability between simulations would also be assured.

10 Acknowledgments

We thank, in addition to support from SKB, also Jan-Erik Lundquist, SMHI, for information on ice data, and Alexander Sokolov, Stockholm University, for helping us work with the massive meteorological data arrays. The latter person is also the programmer responsible for the excellent graphical facilities that most of the presented simulation pictures have benefited from usage. The ÖG area initial fields were prepared by a program developed by Alexander Andrejev and we are indebted to him for this contribution.

Lars Brydsten, Umeå University, has shared his expertise by providing the ÖG area bathymetric grid. He has also been of highly appreciated assistance with other queries concerning geological and geographical issues. Fredrik Wulff, Stockholm University, is thanked for granting permission to use the gridded atmospheric data and Bo Gustafsson from the Oceanographic Institute of Göteborg University also deserves thanks for supplying them.

Linda Johansson, Martin Isæus, Regina Schüldt and Tobias Lindborg, all members of the BIOSAFE work group, have contributed with finding references or by other helpful activities and are all thanked collectively.

Finally we owe a deeply felt gratitude to Ida Engqvist and Tonya Andrejev. Without their support and assistance this project could not have been brought to a conclusion in the time allotted.

11 References

Andersson J & Hillgren R, 1992 SMHI:s undersökningar utanför Forsmark 1992 (The investigations by SMHI outside Forsmark 1992; in Swedish). SMHI Oceanografi rapport No. 57. 14 pp.

Andersson J, Riggare P & Skagius K, 1998a Project SAFE – Update of the SFR-1 safety assessment Phase 1. SKB-R-98-43.

Andersson J, Riggare P & Skagius K, 1998b Project SAFE – Update of the SFR-1 safety assessment Phase 1 Appendices. SKB-R-98-44.

Andrejev, O & Sokolov A, 1989 Numerical modelling of the water dynamics and passive pollutant transport in the Neva inlet. Meteorologia i Hydrologia, 12, 78–85, (in Russian).

Andrejev O & Sokolov A, 1990 3D baroclinic hydrodynamic model and its applications to Skagerrak circulation modelling. 17th Conf. of the Baltic Oceanographers, Proc., 38–46, 23, 280–287.

Bergström S and Carlsson B, 1994 River runoff to the Baltic Sea: 1950–1970. Ambio 23, 280–287.

Bolin B & Rodhe H, 1973 A note on the concepts of age distribution and transit term in natural reservoirs. Tellus, 25, 58–62.

Brydsten L, 1999 Shore level displacement in Öregrundsgrepen. SKB-TR-99-16, Swedish Nuclear Fuel and Waste Mngt Co., Stockholm.

Bunker J, 1977 Computations of surface energy flux and annual air-sea interaction cycle of the North Atlantic. Mon. Weather Rev., 105, No. 9.

Csanady G T, 1982 Circulation of the coastal ocean. D Reidel Publ. Co. Boston. 279 pp.

Engqvist A, 1990 Accuracy in material budget estimates with regard to temporal and spatial resolution of monitored factors. Estuarine, Coastal & Shelf Science 30: 299–322.

Engqvist A, 1993 Water turnover in Örefjärden, 1991. Aqua Fennica, 23, 17–27.

Engqvist A, 1996 Long-term nutrient budgets in the eutrophication of Himmerfjärden estuary. Estuarine, Coastal & Shelf Science, 42, 483–507.

Engqvist A, 1997 Water exchange estimates derived from forcing for the hydraulically coupled basins surrounding Äspö island and adjacent coastal water. SKB-TR-97-14.

Engqvist A, 1999 Estimated retention times for a selection of coupled coastal embayments on the Swedish west, east and north coasts. Swedish EPA report 4910. 22 pp.

Engqvist A & Omstedt A, 1992 Water exchange and density structure in a multi-basin estuary. Continental Shelf Research, 12: 1003–1026.

Evans, 1985 A box model for calculation of collective dose commitment from radioactive waterborne releases to the Baltic Sea. J. Environ. Radioactivity, 2, 41–57.

Gidhagen L & Rahm L, 1990 Water exchange and dispersion modelling in coastal regions: A method study. Vatten, 46, 7–17.

Gidhagen L, Nyberg L & Rahm L, Unpubl. A framework for a coastal dispersion model. 19 pp.

Gidhagen L, Rahm L and Nyberg L, 1989 Lagrangian modelling of dispersion, sedimentation and resuspension processes in marine environments. Dt. Hydrogr. Z., 42, 249–270.

Gustafsson B, 1997 Time-dependent modelling of the Baltic entrance area. Part I: Qantification of circulation and residence times in the Kattegat and the straits of the Baltic sills. In: Dynamics of the seas and straits between the Baltic and north seas. Diss. Thesis. Earth Sciences Centre, Dept. of Oceanography. Göteborg University. 41 pp.

Hemström B, 1993 Forsmark – Strömmätningar och beräkningar för modifierat kylvattenintag. (Forsmark – Current measurement and computations for modified cooling water intake; in Swedish) Vattenfall Utveckling AB report No. VU93:B2. 33 pp.

Lam D C L, Murthy C R & Simpson R B, 1984 Effluent transport and diffusion models for the coastal zone. Lecture notes on Coastal and Estuarine studies No. 5. Springer-Verlag. New York. 168 pp.

Lane A & Prandle D, 1996 Inter-annual variability in the temperature of the North Sea Continental Shelf Res., 16, 1489–1507.

Lindell, T & Kvarnäs H, 1978 Vattenomsättning i djuphålorna utanför Forsmark. (Water turnover in the isolated depths outside Forsmark; in Swedish). 10 pp.

Liu S-K and Leendertse J J, 1978 Multidimentional numerical modellling of estuaries and coastal seas. Adv. Hydrosci., 11, 95–164.

Lundqvist J-E & Årnell T, 1992 A summary of the ice season and icebreaking activities 1991/92. SMHI, Norrköping. 45 pp.

Marchuk G I, 1980 Numerical mathematical methods. Nauska. Moscow. 536 pp. (in Russian).

Mesinger F & Arakawa A, 1976 Numerical methods used in atmosperic models. GARP publications series, No 17, Vol. I. 64 pp.

Mattson J, 1987 Analysis of the exchange of salt between the Baltic and the Kattegat through the Öresund using a three-layer model. J. Geophys. Res. 101:C7, 16571–16584.

Millero F & Kremling I K, 1976 The densities of Baltic waters. Deep-Sea Res. (23) 611–622.

Omstedt A, 1990 A coupled one-dimensional sea ice-ocean model applied to a semi-enclosed basin. Tellus, 42a, 568–582.

Omstedt A, 1998 Freezing estuaries and semi-enclosed basins. Physics of ice-covered seas, 2, 483–516.

Omstedt A, 1999 Forecasting ice on lakes, estuaries and shelf seas. In: J S Wettlaufer, J G Dash and N Untersteiner (Eds.) Ice physics and the natural environment, NATO ASI Ser., Vol. I 56. Springer-Verlag, Berlin. pp. 185–207.

Patten B C, 1968 Mathematical models of plankton production. Int. Revue ges. Hydrobiol., 53, 357–408.

Persson J, Wallin M & Wallström K, 1993 Kustvatten i Uppsala Län 1993. (Coastal water in the County of Uppsala 1993; in Swedish). Ord & Form AB, Uppsala. 246 pp.

Simons T J, 1974 Verification of numerical models of Lake Ontario, Part 1 Circulation in spring and early summer. J. Phys. Oceanogr., 4, 507–523.

Sokolov A, Andrejev O, Wulff F & Rodriguez-Medina M, 1997 The data assimilation system for data analysis in the Baltic Sea. System Ecology contributions No. 3 Dept. Systems Ecology, Stockholm Univ. 66 pp.

Spalding D B, 1981 A general purpose computer program for multi-dimensional one- and two-phase flow. J. Math. and Comput. in Simulation, 23, 267–276.

Stigebrandt A, 1990 On the response of the horizontal mean vertical density distribution in a fjord to low-frequency density fluctuations in the coastal water. Tellus, 42A, 605–614.

Stigebrandt A and Wulff F, 1987 A model for the dynamics of nutrients and oxygen in the Baltic Proper. J. Mar. Res., 45, 729–759.

Sundblad B, Appelgren A, Bergström U, Edlund O & Wilkens A-B, 1983 Referensutsläpp för Forsmarksverket, Version 2. (Reference discharge of the Formark plant, Version 2; in Swedish). Studsvik report/NW-83/573. 90 pp.

Söderkvist J, 1997 Water exchange in a shallow bay. Dept. of Oceanography, Göteborg University. ISSN 1400-3821. 24 pp.

Tennekes H & Lumley J L, 1972 A first course in turbulence. The MIT Press. Cambridge. 300 pp.

UNESCO, 1985 The international system of units (SI) in oceanography, UNESCO Technical Papers No. 45. IAPSO Pub. Sci. No. 32, Paris, France.

ISSN 1404-0344

CM Gruppen AB, Bromma, 1999